

Structural Parameters of Dwarf Galaxies in the Coma Cluster: On the Origin of dS0 Galaxies.

J. A. L. Aguuerri

Instituto de Astrofísica de Canarias, C/ Vía Láctea s/n, 38205 La Laguna, Spain

J. Iglesias-Páramo

*Laboratoire d'Astrophysique de Marseille, BP8, Traverse du Siphon, 13376 Marseille,
France*

Instituto de Astrofísica de Andalucía, Apdo. 3004, 18080 Granada, Spain

J. M. Vílchez

Instituto de Astrofísica de Andalucía, Apdo. 3004, 18080 Granada, Spain

and

C. Muñoz-Tuñón & R. Sánchez-Janssen

Instituto de Astrofísica de Canarias, Vía Láctea s/n, 38205 La Laguna. Spain.

ABSTRACT

In this paper we analyze the structural parameters of the dwarf galaxies in the Coma cluster with $-18 \leq M_B \leq -16$ and classify them in two types: those with surface brightness profiles well fitted by a single Sersic law were called dwarf ellipticals (dEs), and those fitted with Sersic-plus-exponential profiles were classified as dwarf lenticulars (dS0s). The comparison of the structural parameters of the dwarf galaxies in the Coma and Virgo clusters shows that they are analogous. Photometrically, the dE and dS0 galaxies in Coma are equivalent, having similar colors and global scales. However, the scale of the innermost parts (bulges) of dS0 galaxies is similar to the bulges of late-type spiral galaxies. In contrast, dEs have larger scales than the bulges of bright galaxies. This may indicate that dS0 and dE galaxies have different origins. While dE galaxies can come from dwarf irregulars (dIs) or from similar processes as bright Es, the origin of dS0 galaxies can be harassed bright late-type spiral galaxies.

Subject headings: galaxies: dwarf — galaxies: evolution — galaxies: clusters: general

1. Introduction

Dwarf galaxies are the most numerous type of galaxies in the Universe. The term dwarf is applied to galaxies with low central surface brightness and with luminosities below $M_B = -18$. According to the hierarchical theory of galaxy evolution, dwarfs are the building blocks of the brightest galaxies. We can distinguish two main classes of dwarf galaxies: dwarf ellipticals (dEs) and dwarf Irregulars (dIs). These low mass systems have similar stellar distributions, both in terms of functional form and in terms of typical central surface brightness and scale lengths (Lin & Faber 1983; van Zee et al. 2004a). In general, their surface brightness profiles can be well fitted by Sersic (1968) profiles, with shape parameter $n \approx 1\text{--}2$ (Barazza et al 2003; Graham & Guzmán 2003). However, some of the dE galaxies show a nucleus in the center of the object that is well fitted by a Gaussian point-like source (Graham & Guzmán 2003). Both types also follow the same luminosity–metallicity relation (Skillman et al. 1989; Richer & McCall 1995). Nevertheless, they differ in gas content and the age of their stellar populations, dIs being gas-rich galaxies with active star formation (Patterson & Thuau 1996; van Zee et al. 2001) in contrast with dEs, which are gas-poor objects with an old and evolved stellar population. These differences in gas content and the star formation are also presented in the typical broad-band colors of these objects. Thus, dI galaxies typically have $B - R \approx 1$ and dEs $B - R \approx 1.5$ (Trentham 1998).

Sandage & Binggeli (1984) observed that the surface brightness profiles of some of the dE galaxies in Virgo cluster could not be fitted with a single component. Binggeli & Cameron (1993) fitted an exponential profile to the outermost regions of the surface brightness of these galaxies, but this clearly cannot fit their surface brightness profiles at all radii, which indicates that these objects have at least two photometric components. They called these types of objects dwarf lenticular (dS0) galaxies. These galaxies are also gas-poor systems and have an evolved and old stellar population, with colors typical of dE galaxies, but they present higher flattening (Binggeli & Popescu 1995). It has recently been discovered that some of the dS0 galaxies in Virgo cluster have a disk-like structure, due to the presence of bars or/and spiral patterns (Jerjen et al. 2000; Barazza et al. 2002).

In the standard picture, dwarf galaxies are formed from the gravitational collapse of primordial density fluctuations. Once the first stars are formed, mechanisms of energy feedback into the interstellar medium are proposed in order to regulate the subsequent star formation or even change in the structure of the galaxy (Dekel & Silk 1986). It has been observed by several authors in the past that the structural parameters of dEs and bright E galaxies follow a continuous and global relation. This argument has been used in order to infer a common formation process for dE and bright E galaxies, dEs being the genuine low luminosity extension of giant E galaxies (Binggeli 1985; Jerjen & Binggeli 1997; Graham & Guzmán

2003). In contrast, other authors, on the basis of a similar stellar distribution of dE and dI galaxies, have suggested the presence of linked evolutionary scenarios between both types of galaxies (Lin & Faber 1983; Kormendy 1985; Caldwell & Bothun 1987; Binggeli & Cameron 1991). This last framework has been reinforced by recent kinematic studies of dE galaxies in the Virgo cluster (Pedraz et al. 2002; Geha et al. 2002; Geha et al. 2003; van Zee et al. 2004a). It was found that most of the dE galaxies are rotationally supported in a similar to dIs. This indicates that dE galaxies can be evolved dIs that have lost their gas content. The important question is then how or why dI galaxies stopped their star formation and lost their gas content. Several physical mechanisms have been proposed for sweeping the gas and stopping the star formation in a dI galaxy to produce a dE. These can be classified into internal (kinetic energy from supernova explosions; Dekel & Silk 1986; De Young & Gallagher 1990) or external processes (related with environmental processes in high density environments like galaxy clusters; Lin & Faber 1983; van Zee et al. 2004a,b). The former explanation, however, deserves more detailed modeling. As shown in Silich & Tenorio-Tagle (2001), more parameters, such as the structure of the host galaxy, have to be taken into account in order discover the likely fate of the material processed in the starbusts.

Galaxies in high density environments, like galaxy clusters, evolve through many different physical processes; e.g., harassment (Moore et al. 1996), ram-pressure stripping (Gunn & Gott 1972; Quilis et al. 2000), tidal effects and mergers (Toomre & Toomre 1972; Bekki et al. 2001; Aguerri et al. 2001) or starvation (Bekki et al. 2002). In Aguerri et al. (2004) it was shown that bright spiral galaxies in the Coma cluster present smaller disk scale-lengths than equivalent field galaxies. This was explained in terms of the harassment suffered by the galaxies in Coma while they are falling into the cluster. But the above cited physical mechanisms not only play an important role in the evolution of bright galaxies, they can even strongly affect the evolution of dwarf galaxies. They are mostly located in galaxy clusters, being more common in lower density environments (Phillips et al. 1998, Pracy et al. 2004; Sánchez-Janssen et al. 2005), which indicates that there is a link between the dwarf population and the cluster environment. Van Zee et al. (2004a) argued that the evolution from dIs to dE galaxies was mostly driven by the gas stripping mechanism. Thus, dI galaxies falling into the cluster potential lose their gas content by shock with the hot intracluster medium, evolving into dE galaxies. This mechanism can explain why dIs and dEs have similar scales, as well as the rotation features recently observed in some dE galaxies. This scenario could also explain the evolution of dIs into dE galaxies without rotation features. As demonstrated by Mayer et al. (2001a,b), repeated tidal interactions suffered by a dwarf satellite galaxy can remove the kinetic signature and transform a dI galaxy into a dE. But more than one single mechanism can drive this evolution, it being difficult to distinguish which of them is the dominant one. Recently, the development of numerical simulations have provided a way of

following the evolution of galaxies in cluster-like potentials (Moore et al. 1996, 1998, 1999, 2000). The main conclusion of these studies is that the morphological evolution of galaxies in clusters is driven, on short timescales, by the interactions between galaxies and by the gravitational cluster potential. The cumulative effect of these encounters can cause a dramatic morphological transition between late type spiral galaxies to dwarfs (Moore et al. 1996). This has been recently confirmed by Mastropietro et al. (2004), who have studied the evolution of a late-type galaxy in a galaxy cluster simulation and found that the galaxies undergo significant transformations, moving through the Hubble sequence from late type to dwarf galaxies. So, this could be another mechanism for the formation of dwarf galaxies in clusters. In this paper we analyze the structural parameters of a sample of dwarf galaxies in the Coma cluster and study their relation with the different evolutionary scenarios described.

The population of dwarf galaxies in Coma has been extensively studied in the literature, but most of these researches are related with properties of their luminosity function (Thompson & Gregory 1993; Trentham 1998; Iglesias-Páramo et al. 2002; Mobasher et al. 2003), or their color and stellar population analysis (Secker et al. 1997; Trentham 1998; Poggianti et al. 2001). In contrast to other nearby clusters like Virgo, very little is reported in the literature about the structural parameters of dwarf galaxies in Coma. Graham & Guzmán (2003) have recently published the structural parameters of a sample of 16 dwarf galaxies in Coma using *HST* images. Previous studies of morphology in the Coma cluster galaxies do not reach the dwarf luminosities (Andreon et al. 1996, 1997). Only Gutierrez et al. (2004) give the quantitative morphology of Coma galaxies down to $M_B = -16$, but restricted to the central 0.25 deg^2 region. In the present paper we present the largest study of structural parameters for dwarf galaxies in Coma. We have analyzed all dwarf galaxies with luminosities brighter than $M_B = -16$, located in an area of 1 deg^2 around the center of the cluster.

This paper is organized as follows. In Section 2 we present the sample of dwarf galaxies analyzed. The fit of the surface brightness profiles of the objects is shown in section 3. The correlation between the structural parameters and the comparison with dwarf galaxies in Virgo are shown in Section 4. The discussion is presented in Section 5, and conclusions are given in Section 6. Through this paper we will assume $H_0 = 75 \text{ km s}^{-1} \text{ Mpc}^{-1}$.

2. Observations and Sample Selection

The observations were taken with the Wide Field Camera (WFC) at the prime focus of the 2.5 m Isaac Newton Telescope (INT) at the Roque de los Muchachos Observatory (La Palma), in 2000 April. The plate-scale of the CCD was $0.333 \text{ arcsec/pixel}$, and the seeing of

the images was about $1.5''$.

Although a detailed description of the observations, data reduction, calibration and extraction of the objects are given in Iglesias-Páramo et al. (2002, 2003), a brief summary is given here. Four fields of the Coma cluster were obtained in photometric conditions, covering an area of $\approx 1 \text{ deg}^2$ in the North-East region of the cluster, coinciding with the central part of the Godwin catalog of the Coma cluster (Godwin et al. 1983). Three different exposures of 300 s each, slightly dithered, to remove cosmic rays, were obtained for each field. The data reduction of the images was carried out using standard IRAF tasks, and the images were astrometrized using the United States Naval Observatory (USNO) catalog of stars. After the calibration of the images, typical errors (Poisson and zero point uncertainty) in the magnitude of the objects were about 0.15 mag.

We have selected as dwarf galaxies those with apparent magnitude brighter than $m_r = 17$, absolute magnitude fainter than $M_B = -18^1$, and belonging to the Coma cluster. The limiting magnitude $m_r = 17$ was taken based on Monte Carlo simulations, in order to determine the limiting magnitude for a reliable measurement of the structural parameters of the galaxies (see Aguerri et al. 2004). We have obtained the recessional velocities and the B band magnitudes of the objects from Godwin et al. (1983) catalog. We considered as Coma cluster members those galaxies with $4000 \leq cz \leq 10000$. This gives a total number of 99 objects with absolute magnitudes in the range $-16 \leq M_B \leq -18$. All the galaxies selected in this study have a color $B - R > 1.25$. This is the typical color shown by an evolved and old stellar population like that of dE galaxies (see Graham & Guzmán 2003).

We fitted ellipses to the isophotes of all the sample, using the IRAF task ELLIPSE. This provides the radial surface brightness profiles of the objects, which were then fitted by mathematical functions (see Section 3). In 15% of the galaxies we could not fit the isophotes, because these objects were located very close to a bright galaxy or field star, and no reliable photometry could be obtained for them.

3. Fit of the Surface Brightness Profiles

The surface brightness profiles of the objects were fitted using a Sersic or Sersic+exponential profiles. The Sersic profile is given by the law (Sersic 1968):

¹The adopted distance modulus of the cluster was -34.83, this was obtained assuming a recessional velocity of 6925 km s^{-1} obtained from NASA Extragalactic Database (NED)

$$\mu(r) = \mu_e + 2.5 \times b_n \left(\left(\frac{r}{r_e} \right)^{1/n} - 1 \right), \quad (1)$$

where r_e is the effective radius, which encloses half of the total luminosity of the profile, μ_e is the effective surface brightness, and n is the profile shape parameter. The parameter b_n is given by $b_n = 0.868n - 0.142$ (Caon et al. 1993).

The exponential profile is given by (Freeman 1970):

$$\mu(r) = \mu_0 - 1.0857 \times r/h, \quad (2)$$

where μ_0 is the central surface brightness and h is the scale length of the profile.

The free parameters of the models were fitted using a Levenberg–Marquardt nonlinear fitting routine and were determined by minimizing the χ^2 of the fit. We have used the algorithm designed by Trujillo et al. (2001a). This algorithm takes into account the seeing effects on the surface brightness profiles (Trujillo et al. 2001b,c) and the intrinsic ellipticity of the galaxies. It has been successfully applied in previous studies of the quantitative morphology of galaxies in nearby clusters (Trujillo et al. 2002; Gutierrez et al. 2004; Aguerri et al. 2004), medium redshift clusters (Trujillo et al. 2001a), and field galaxies (Aguerri & Trujillo 2002; Trujillo & Aguerri 2004).

Extensive Monte Carlo simulations were carried out in order to determine the uncertainties in the determination of the structural parameters. We simulated galaxies with structural parameters similar to the observed objects. These simulations tell us that the structural parameters of simulated objects with two components can be obtained within errors less than 20% for those objects with magnitudes brighter than $m_r = 17$. Objects modeled with only one component can be recovered with errors less than 20% until $m_r = 19$, (see the simulations presented in Aguerri et al. 2004).

All the galaxies were first fitted with a single Sersic profile. If the residuals from this fit (taking into account the photometric errors in the surface brightness profiles) were always less than 0.15 mag arcsec $^{-2}$, then we took such fit as a good one. Those galaxies with larger residuals were fitted with two components (Sersic+exponential). Figure 1 shows, as an example, the fits and residuals of two galaxies. It can be seen that the fits of those objects with one component have very large residuals in the outermost regions of their surface brightness profiles. In contrast, the residuals were reduced when two components were fitted. This fitting procedure ensures a fit to the surface brightness profiles of the galaxies using the smallest number of components.

The galaxies were classified according with the number of fitted components. Those

well fitted by a single Sersic profile, were called dE galaxies, and those fitted with Sersic+exponential profiles were called dS0 galaxies. The result was 55 objects classified as dEs and 29 as dS0 galaxies. Tables 1 and 2 show the structural parameters of the dE and dS0 galaxies. Figures 2 and 3 show the fit of the surface brightness profiles of the galaxies and the residuals.

3.1. Comparison with previous studies

The goodness of the fit of the surface brightness profiles of our galaxies can be analyzed by comparing the aperture magnitude of the objects obtained with SExtractor (Bertin & Arnouts 1996), and those computed from the fitted models in this work. This comparison is showed in Fig. 4, where it can be seen that the agreement between both magnitudes is very good in all cases.

The structural parameters of dwarf galaxies in the Coma cluster have not been extensively studied in the literature. Actually, there are only two previous works with which we can compare our results: Gutierrez et al. (2004) and Graham & Guzmán (2003).

Gutierrez et al. (2004) obtained the structural parameters of Coma galaxies located in the central part (0.25 deg^2) of the cluster down to $m_r = 17$. They used the same code for fitting the surface brightness profiles, but, their classification of the galaxies was slightly different.² We have 53 galaxies in common with the Gutierrez et al. (2004) sample. The same classification in both samples is achieved in 74% of the common objects. The mean errors of the structural parameters for those galaxies are less than 20%, which is the typical error obtained from the simulations for the structural parameters of these objects (see Aguerri et al. 2004). For the rest, 12 were classified as dS0s by Gutierrez et al. (2004), but our fits prove that only one Sersic profile is a good fit for those objects. Two of them, GMP 3126 and GMP 3463, have structure in the outermost part of the surface brightness profiles, and only the inner regions of the profiles were fitted, and two more (GMP2615, GMP 2778) have unreliable parameters in Gutierrez et al. (2004). If we exclude this four galaxies, them we have the same classification in both samples for the 80% of the common galaxies. There are also two galaxies (GMP 3017 and GMP 3707) classified as dEs by Gutierrez et al. and as dS0s in this study. But, for these two galaxies one component can not fit the external parts of their surface brightness profiles. For this reason we include a second component in the fit.

²Gutierrez et al. (2004) fitted all the galaxies with two components (Sersic+exponential), and those with a bulge-to-disk (B/T) ratio larger than 0.6 or not well fitted with two components were fitted with a single Sersic profile.

It should be noticed that the inclusion of a second component in the fits would reduce the χ^2 and the residuals of the fits due to the addition of more free parameters. We have only fitted a second component in those cases where the residuals were very large, especially in the outermost regions of the profiles. This means that the number of dS0 galaxies classified in this study is a lower limit. It is possible that some of the galaxies classified as dEs have two components. Future kinematic studies of these objects will shed some light on this problem.

There is another important difference from Gutierrez et al. (2004). Although we have used the same code for the decomposition of the surface brightness profiles of the galaxies, we have not used the same images. This means that we have not fitted the structural parameters of the galaxies to the same surface brightness profiles. Variations in the sky background level of about 1–2% can affect to the external parts of the surface brightness profiles of the objects and modify by about 10–20% the fitted structural parameters of the galaxies. This effect is especially important for such faint objects as those studied in the present paper. This is another reason why we have not obtained exactly the same parameters for those galaxies classified as dEs in Gutierrez et al. (2004) and the present paper.

We have five galaxies in common with Graham & Guzmán (2003). GMP 2960 and GMP 3292 were classified in our and Graham & Guzmán (2003) samples as dS0. The differences in the parameters for GMP 2960 are about 30%. GMP 3292 has larger differences in the parameters of the bulge component because Graham & Guzmán (2003) fitted a Gaussian profile in the innermost region of this galaxy; the disk is very similar to our fitted disk. The galaxies GMP 2879 and GMP 2985 were fitted with single Sersic profiles in both samples, and the mean error in the structural parameters is less than 20%. We have fitted the galaxy GMP 3486 with a single Sersic profile, while Graham & Guzmán (2003) fitted it with a two component fit. But, our fit demonstrates that the residuals of the fit are good enough with only one component. The differences of the fitted structural parameters for the galaxies in common with Graham & Guzmán (2003) could be due to the high resolution and small background level of the *HST* images.

3.2. Contamination of the sample

Because of their low luminosity, the classification of these objects is not easy. As mentioned before, the sky background subtraction or the presence of close companions can influence the fit of the surface brightness profiles and the fitted structural parameters of the objects. There is a further concern about the selection of the sample related on the fact that we can also have some level of contamination by spirals due to the uncertainty in the Coma cluster distance and the depth of the cluster. Spiral galaxies located at the back of

the cluster or in the background might be taken as dS0s at the front of the cluster. We have visually checked out the images of the dS0 galaxies (see Fig. 5) in order to reduce the possible contamination by spirals. It can be seen that only one galaxy (GMP 2914) can be a spiral galaxy, instead of a dS0. This galaxy shows low surface brightness spiral arms and a strong twist of the inner and outer isophotes. The rest of the galaxies in the sample show no signs of spiral structure.

In order to test how the results presented here depend on the classification of the galaxies, we have selected a subsample of dS0 galaxies. They are the 12 objects with the highest values of χ^2 for the fits of their surface brightness profiles by only one Sersic component. These objects are classified in our sample and Gutierrez et al (2004) sample as galaxies with two photometric components. These will be called the "more reliable sample" and will be shown with larger symbols in all plots where dS0 galaxies will be plotted. We have excluded from this sample the possible spiral galaxy GMP 2914.

4. Correlations among the structural parameters

4.1. Comparison with dwarf galaxies in the Virgo cluster

The quantitative morphology of dwarf galaxies in Virgo has been investigated previously by several authors in the literature. We have compared the structural parameters of dEs in the Coma cluster with those in the Virgo cluster given by Durrell (1997), Barazza et al. (2003) and van Zee et al. (2004a,b). Figure 6 shows r_e , n and $\mu_{o,R}$ as function of the B -band absolute magnitude for dE galaxies in the Coma and Virgo clusters. It can be seen that Virgo and Coma dE galaxies share the same locus in the plots for the common magnitude interval of the data: $-17 \leq M_B \leq -16$. We have run 2D Kolmogorov–Smirnov (KS2D) tests in order to compare the distribution of our data with that in the literature for Virgo cluster (also shown in Figure 6). In all cases the tests give that the distributions of points in the magnitude interval $-17 \leq M_B \leq -16$ are not statistically different. Figure 5 also shows a trend in the structural parameters of dEs. Thus, fainter dE galaxies have smaller r_e and n , and show fainter μ_o . The Pearson correlation coefficients (r) of $r_e - M_B$, $n - M_B$ and $\mu_o - M_B$ relations are: -0.30 , -0.42 , and -0.13 , respectively. The significance of the correlations³ (P) are: 0.002 , 0.001 , and 0.17 , respectively.

The comparison of the structural parameters of our dS0 galaxies and those in the Virgo

³The significance of the correlation is the probability that $|r|$ should be larger than its observed value in the null hypothesis.

cluster from the literature is difficult because of the different fitting techniques used for fitting their surface brightness profiles. Binggeli & Cameron (1993) fitted an exponential profile in the external parts of the surface brightness of the dS0 galaxies in Virgo. We have compared the scale-lengths and central surface brightness of the exponential fits of Binggeli & Cameron (1993) for dS0s in Virgo with the scale-lengths and central surface brightness of our exponential component in our dS0 galaxies in the Coma cluster. Figure 7 shows the results.⁴ It can be seen that, in the common magnitude bin of the two samples, dS0s from Virgo and Coma, have similar scale-lengths and central surface brightness of the exponential component. Figure 7 also shows that fainter dS0 galaxies show smaller scale-lengths for the exponential component. This is also true when we consider only the more secure sample of dS0 galaxies. The coefficients r and P of this relation are: -0.50 , 0.001 , respectively. For the more reliable sample of dS0 galaxies these coefficients are -0.58 and 0.001 , respectively. The central surface brightness does not depend of the absolute magnitude of the galaxy, being $\langle \mu_{o,B} \rangle = 22.50$ mag. arcsec $^{-2}$, and $\sigma = 0.89$. There are five galaxies (three from Coma and two from Virgo) which have $\mu_{o,B} \geq 23.5$ mag arcsec $^{-2}$. They also show very large scale-lengths for the disks. These galaxies are compatible with being LSB galaxies (de Blok et al. 1995). If we do not consider these five galaxies then the mean central surface brightness of the galaxies is $\langle \mu_{o,B} \rangle = 22.24$ mag. arcsec $^{-2}$, and $\sigma = 0.58$. If we consider the more reliable sample of dS0 galaxies in Coma and the Virgo galaxies without the LSBs, then we obtain: $\langle \mu_{o,B} \rangle = 22.43$ mag. arcsec $^{-2}$, and $\sigma = 0.79$. The fact that the central surface brightness of the exponential profiles of dS0 galaxies does not depend on the luminosity of the galaxy is similar to what happened with the disks of bright spirals (Freeman's law). This could indicate that the exponential components of dS0 galaxies are disk-like structures similar to those shown by bright spirals.

Binggeli & Popescu (1995) determined the mean ellipticity of dE and dS0 galaxies in Virgo as 0.30 ± 0.02 and 0.37 ± 0.06 , respectively. These numbers are in very good agreement with the mean ellipticity for dEs and dS0s in Coma obtained from our data: 0.26 ± 0.02 ⁵, and 0.34 ± 0.03 , respectively. The more reliable sample of dS0 has a mean ellipticity of 0.36 ± 0.05 . Thus, dS0 galaxies in the Coma cluster, as was the case for those in Virgo, are flatter objects than dEs.

⁴The B -band central surface brightness of our exponential fits was obtained from the $B - R$ color of the galaxies.

⁵Unless it stated to the contrary, all the errors showed in this paper in the value of all mean quantities are the errors of the mean. They were computed as the mean value of the quantity divided by the square root of the number of elements.

4.2. Comparison of dE/dS0 with bright galaxies in Coma

Comparison of the structural parameters of the dEs and bright Es in the Virgo and Fornax clusters have been used in the past to argue about the different or same formation processes of these two systems of galaxies. Kormendy (1985) found a discontinuity between the structural parameters of dEs and bright E galaxies in Virgo and Leo, concluding that dEs are very different from the sequence of bright E galaxies. A decade later, Jerjen & Binggeli (1997) observed a continuous relation between the Sersic profile shape parameter and the absolute magnitude from dE to bright E galaxies in the Virgo cluster. Based on this relation, they concluded that dEs are the low luminosity version of bright E galaxies. Graham & Guzmán (2003) made a compilation of data from the literature for dE and bright E galaxies from Virgo, Fornax, Leo and 16 dEs from the Coma cluster. They concluded that the discontinuity observed by Kormendy (1985) in the structural parameters of dE and bright E galaxies was caused by the selection effect of the sample and found a continuous and smooth change in the structural parameters from dE to bright E galaxies, which suggests a common physical formation processes.

Figure 8 shows the relations of the structural parameters of dE and bright E galaxies (from Aguerri et al. 2004) in the Coma cluster. Those relations are obtained with one of the largest (93 galaxies from Coma) and most homogeneous (all the structural parameters have been obtained in the same way) samples available so far in the literature. It can be seen that dE galaxies exhibit fainter μ_o and smaller values of r_e and n than bright E galaxies. The two galaxies which are outside the relations are the two cD galaxies located in Coma. If we remove the two cD galaxies from the relations, the Pearson coefficients of $r_e - M_R$, $n - M_R$ and $\mu_o - M_R$ relations are -0.51 , -0.58 , and -0.65 , respectively, in all cases with $P < 0.001$. These relations suggest that bright E and dE galaxies form a continuous family of objects with similar physical formation processes.

We have also computed the mean ellipticity of bright elliptical galaxies in Coma from Aguerri et al. (2004), as 0.25 ± 0.02 . This shows that dE and bright E galaxies in the Coma cluster have similar ellipticities. Figure 9 shows the cumulative distribution function of the ellipticities of dE, dS0, and E galaxies in the Coma cluster. The cumulative distribution function of dEs and Es is very similar for galaxies with ellipticities less than 0.3, being different for galaxies with ellipticities greater than 0.3. Nevertheless, the KS test reveals that we cannot statistically exclude the possibility that that Es and dEs have the same distribution function. On the contrary, the KS test tells us that dS0s have a different distribution function of ellipticities from E and dE galaxies.

We have classified as dS0 galaxies those objects with surface brightness profiles fitted with two components (see Section 3): one Sersic profile which dominates the innermost

regions of the surface brightness profiles (similar to the bulge in bright spiral galaxies) and another exponential profile which dominates in the outermost regions (similar to the disks of the bright spirals). Because of this similarity between dS0s and bright spirals we have compared the structural parameters of the bulges and disks of bright spiral galaxies in Coma (Aguerri et al. 2004) with the Sersic and the exponential profiles of dS0s, respectively. Figures 10 and 11 show this comparison. Figure 10 shows that there is a continuous relation for the scales of the exponential profiles of dS0s and the disks of bright spirals: brighter galaxies have disks with larger scale-lengths. The coefficients r and P of this relation are -0.63 and 0.001 , respectively. These coefficients are -0.66 and 0.001 for the more reliable sample of dS0 galaxies. The central surface brightness of the disks of bright spirals does not depend on the absolute magnitude of the galaxy. This is the well known Freeman law, discovered by Freeman (1970) for bright spiral galaxies. The mean central surface brightness of the disks of bright galaxies in Coma obtained from our data is $\langle \mu_{o,R} \rangle = 19.76$ mag arcsec $^{-2}$ and $\sigma = 0.90$. Neither does the central surface brightness of the exponential profiles of dS0 galaxies depend on the luminosity of the galaxy, the mean value being $\langle \mu_{o,R} \rangle = 20.76$ mag arcsec $^{-2}$ and $\sigma = 0.99$, and $\langle \mu_{o,R} \rangle = 20.39$ mag arcsec $^{-2}$, and $\sigma = 0.80$ for the more reliable sample of dS0 galaxies (see Fig. 10). Both values differ by only 1σ . The structural parameters of the Sersic profiles of dS0s and bulges of bright Coma galaxies as a function of the R -band absolute magnitude of the galaxies are shown in Figure 11. It can be seen that there is a correlation between the Sersic shape parameter (n), the effective radius (r_e), and the bulge central surface brightness μ_o . Brighter galaxies have bulges with larger n , r_e , and brighter μ_o . The Pearson coefficients of $r_e - M_R$, $n - M_R$ and $\mu_o - M_R$ relations are -0.47 , -0.27 , 0.32 , respectively. The P coefficients of the relations are: 0.001 , 0.018 , 0.005 , respectively. The Pearson coefficients of those relations for the more reliable sample of dS0 are -0.53 , -0.20 , and 0.29 , respectively. The P coefficients of the relations are 0.001 , 0.125 , 0.011 , respectively.

These results show that the photometric parameters of the Sersic and exponential components fitted to the surface brightness profiles of dS0 galaxies follow a continuous relation with the photometric parameters of bulges and disks of bright spirals in Coma, respectively. This suggests that the Sersic and exponential photometrical components of the dS0 galaxies are similar bulge-like and disk-like structures to those seen in bright spirals. Similarly to what happens with dE and bright E galaxies, we propose dS0 galaxies as the low luminosity version of bright galaxies.

5. Discussion

We have analyzed the structural parameters of a sample of dwarf galaxies in the Coma cluster that were classified according to the decomposition of their surface brightness profiles. Galaxies called dEs are those whose surface brightness profiles are well fitted with a single Sersic profile. We have termed as dS0 galaxies those dwarf galaxies for whose surface brightness profiles are well fitted with two components (Sersic+exponential). All of these galaxies have colors $B - R \geq 1.25$, typical colors for an evolved and old stellar population.

The selection of the galaxies by the B-R color does not ensure to have a sample free of contamination by spiral galaxies, as spiral galaxies can also have red colors (Driver et al. 1994). Moreover, there is a ≈ 3 magnitude overlap of the type-specific luminosity functions of S0, Sp and dE/dS0 (Binggeli et al. 1988). A visual inspection of the images of the objects has confirmed the presence of one possible spiral (GMP 2914). This object has weak spiral arms, and a strong twist of the isophotes. Nevertheless, this object shows a very red color ($B - R = 1.84$). The presence of only one object as a possible spiral galaxy confirms that the contamination of the sample of dS0 galaxies is not very high, and a selection criteria including visual inspection and measurement of the isophotal twist is enough to discard spirals which might contaminate the sample.

As pointed by many authors for the Fornax and Virgo dwarf galaxies, we have found a continuous relation of the structural parameters for the dE and bright E galaxies in the Coma cluster. This could indicate that dE and bright E galaxies have similar physical formation processes. However, the common relation of the structural parameters of dE and bright E galaxies has been explained by some authors as more due to the uniformity of their dark matter halos (Navarro et al. 1997) rather than to a common formation mechanism. Moreover, it has also been argued in the literature that the similarity of the structural parameters of dI and dE galaxies is also indicative of a common origin between dE and dI galaxies (Lin & Faber 1983). This has been recently reinforced by the finding of substantial amount of rotation for some dE galaxies in Virgo, similar to that shown by dIs (van Zee et al. 2004a). It has been proposed that dEs would be evolved dI galaxies that have lost their gas due to ram pressure stripping with the hot intracluster medium (van Zee et al. 2004a). Although there is much discussion in the literature about the origin of dEs, little is mentioned about dS0s. Usually, dE and dS0 galaxies are taken as galaxies belonging to the same family of objects, those with an old and evolved stellar population. But are they really the same class of objects? What is the origin of dS0 galaxies? Have dS0s and dEs similar formation processes? In order to answer these questions we should compare the structural and kinematic properties of dS0 and dE galaxies in the Coma cluster.

5.1. Comparison between dE and dS0 galaxies in the Coma cluster

5.1.1. Photometric parameters

First, we have compared the typical scales of dS0s and dEs in the Coma cluster. We computed the effective radius of all dwarf galaxies in the same way. This was done from the fitted models of their surface brightness profiles by resolving the equation $L(r_e) = L_T/2$, L_T being the total luminosity of the model. Sersic or exponential profiles have an infinite radial extension, while the observed surface brightness profiles only reach the sky background surface brightness. Thus, we computed the total luminosity of the fitted models with the expression $L_T = 2\pi \int_0^{r_c} r I(r) dr$, where $I(r)$ is the intensity of the profile, and r_c is the truncation radius. The truncation radius adopted for each profile was the radial distance corresponding to an R -band surface brightness of $24.5 \text{ mag arcsec}^{-2}$. This is the typical maximum radial extension of our surface brightness profiles (see Figs 2 and 3). We obtained the following mean r_e of dS0 and dE galaxies in Coma: 2.32 kpc ($\sigma = 0.80 \text{ kpc}$) and 2.83 kpc ($\sigma = 0.95 \text{ kpc}$), respectively. The more secure sample of dS0 show $\langle r_e \rangle = 2.23$ and $\sigma = 0.85$. Thus, within the errors, dEs and dS0s in Coma have similar scales.

We have measured the $B - r$ colors of the dwarf Coma galaxies. The mean $B - r$ color of dE galaxies was 1.78 ± 0.02 (1.75 ± 0.04 for dS0s). The two samples of galaxies have the same mean color within the errors. The KS test shows that we cannot exclude the possibility that the two color distribution of dEs and dS0s comes from the same color distribution. We also analyzed the $B - r$ color of the dE and dS0 galaxies as a function of the position in the cluster. The dE and dS0 galaxies were divided in two families: those located at $R/r_s \leq 2$ and those with $R/r_s > 2$. The $B - r$ color of galaxies at $R/r_s \leq 2$ was 1.79 ± 0.02 and 1.81 ± 0.01 for dEs and dS0s, respectively, while the galaxies located at $R/r_s > 2$ have colors of: 1.80 ± 0.03 and 1.64 ± 0.09 for dEs and dS0s, respectively. Figure 12 shows the color histograms of the galaxies. Although the mean color of dS0 galaxies located in the outer parts of the cluster is bluer than that for those located in the innermost region, the KS test shows that we cannot exclude the possibility that the color distribution of those two families of dS0 galaxies comes from the same distribution. The same happens for dE galaxies located in the inner and outermost regions.

We ran a two dimensional KS test in order to investigate the differences in the spatial distributions between dEs and dS0s in the cluster. The test reveals that we cannot exclude the possibility that dEs and dS0s have the same spatial distribution in the cluster. We have also run the two dimensional KS test for the spatial distribution of dwarfs (dEs and dS0s) and bright galaxies (E/S0 and Sp). The results were that the spatial distribution of dEs is statistically different from bright galaxies (E/S0 and Sp). But, this is not the case for dS0s.

We cannot exclude the possibility that the spatial distribution of dS0 galaxies is different from E/S0 or Sp galaxies. No differences have been found concerning the color and spatial distribution when we consider only the more reliable dS0 sub-sample of galaxies.

The previous results prove that there is not a clear distinction between dE and dS0 in Coma by scale, B-R color or spatial distribution. This was also pointed out by Ryden et al. (1999) for a sample of early-type dwarf galaxies in Virgo. They did not find any combination of parameters from the surface photometry that statistically correlates with the dE/dS0 designation. They only found that dS0 galaxies seem different from the dEs in the ellipticity. The dS0 family may represent the tail of the distribution toward flatter shapes, which is in agreement with what we pointed out in section 4.1.

5.1.2. Kinematic properties

The KS test showed that we cannot exclude the possibility that dEs and dS0s have the same radial velocity distribution. One important kinematic parameter is the velocity dispersion of each type of galaxy in a cluster, which gives information about the orbits of the galaxies (Biviano & Katgert 2004). Figure 13 shows the velocity histograms for bright (E and Sp) and dwarf (dE and dS0) galaxies. We have studied the gaussianity of these velocity distributions by computing their kurtosis (K) and skewness (S). A Gaussian distribution has $K = 3$ and $S = 0$. We have obtained $K - 3 = 0.62, 0.69, 0.65$, and 1.27 , and $S = 0.14, 0.24, 0.08$, and 0.25 for Es, Sp, dEs, and dS0s, respectively. For the more reliable sample of dS0 galaxies we obtained $K - 3 = 1.43$ and $S = 0.04$. It can be seen that dS0 and Sp galaxies have a velocity distribution that deviates more from Gaussian. The others present similar K and S . We have computed the mean velocity and the velocity dispersion of each type of galaxy using three different methods: fitting a Gaussian to the velocity histograms (see Fig. 13), directly measuring the mean and the dispersion of the velocities of each group of galaxies, and using the robust estimator defined by Beers et al. (1990). The results are given in Table 3.

The χ^2 values of the Gaussian fits given in Table 3 tell us that Sp and dS0 galaxies show the smallest Gaussian distribution of velocities, as was also confirmed by the kurtosis and skewness of their velocity distributions. This means that the results obtained by these Gaussian fits are not very reliable. We have also directly computed the mean velocity and velocity dispersion of the different groups of galaxies, and we have run statistical tests⁶

⁶The statistical tests used were the Student's T -statistic and the F -variance test. The first test gives the probability than two distributions have significantly different mean, and the second gives the probability

in order to find which group of galaxies has statistically different mean velocity and/or velocity dispersion from the others. We may conclude that we cannot discard statistically the possibility that all groups have the same mean velocity and velocity dispersion. Nevertheless, it should be noted that the E–dE and Sp–dS0 groups of galaxies give probabilities greater than 0.92 in the F -variance test. This means that there is a hint that the E–dE and Sp–dS0 groups of galaxies have similar velocity dispersions. Beers et al. (1990) proposed a more robust estimator for the computation of the mean velocity and velocity dispersion that does not assume a Gaussian distribution and is optimized for a sample with a small number of objects. It can be seen in Table 3 that the differences in the mean velocity of the different groups of galaxies are smaller than 2σ . Although dS0 and Sp galaxies have slightly higher velocity dispersion than Es and dEs, this difference is also less than 2σ . According with these results, we can then say that there is a hint that dS0 and Sp galaxies have slightly higher velocity dispersion than Es and dEs, but that the difference is not statistically significant.

Biviano & Katgert (2004) found that late type galaxies follow orbits with anisotropic velocity distributions. Although it is not statistically significant, the slightly higher velocity dispersion observed for the group of Sp–dS0 galaxies with respect to the E–dE group could be related to differences in the anisotropy of the orbits. This means that Sp–dS0 galaxies would have more anisotropic orbits than those in the E–dE group. This could be related with infalling motions of the galaxies in the cluster (Solanes et al. 2001). Thus, dS0 galaxies would be objects falling into the cluster following anisotropic orbits, while dEs would be galaxies in isotropic orbits similar to E galaxies.

5.2. Possible formation mechanism of dS0 galaxies

In the previous subsection we have seen the main similarities and differences between dS0 and dE galaxies. We can now try to answer the question about the formation scenario of dS0 galaxies.

One possible explanation could be that dS0s would be an intermediate stage between dI and dE galaxies. In this framework, dI galaxies lose their gas content and cease star formation due to the gas stripping mechanism. The result would be a dS0-like galaxy. Subsequent harassment interactions of the dS0 galaxy with the cluster potential and other galaxies could transform the dS0 into a dE galaxy. The three types of galaxies taking part in the present evolution (dI, dS0 and dE) have similar scales. The physical processes driving the evolution should then imply no change in the scales of their stellar distribution. The gas stripping

that the distributions have different variances.

would drive the evolution from dI to dS0 without change in the stellar distribution because this process affects the gas content of the galaxy but not its stellar content. Nevertheless, the transformation from dS0 to dE should be made by harassment interactions, which affects to the stellar component of the galaxies. It is known that repeated tidal shocks suffered by a dwarf satellite galaxy can remove the kinematic signature of a dI galaxy and transform it into a dE (Mayer et al. 2001a,b), but the final stellar distribution has a typical scale twice as short (Mayer et al. 2001a,b). This means that this framework can hardly explain the similar scales observed in the three types of objects, so dS0 galaxies are not an intermediate step in the evolution from dI to dE galaxies, at least for the observed objects. It could be that dS0 galaxies were stripped dIrrs. But, the presence of two photometric components for dS0s makes this unlikely. Usually, the surface brightness of dIrr galaxies is well fitted with only one Sersic ($n = 1$) profile (van Zee 2000).

In the harassment scenario, dE and dS0 galaxies can be formed by tidal interactions of bright disk spiral galaxies with the gravitational cluster potential and fast galaxy–galaxy encounters (Moore et al. 1996; Mastropietro et al. 2004). Aguerri et al. (2004) found that bright spiral galaxies in the Coma cluster are certainly suffering the effects of harassment: the scale-lengths of the disks of bright spiral galaxies are shorter than those from similar field spirals. Nevertheless, the structural parameters of the bulges of bright spirals in the Coma cluster are not affected. If this picture is correct and most dE or dS0 galaxies are created by this mechanism, then we can think a scene in which dS0 galaxies would be harassed bright spirals that have not lost the disk component completely. In this picture, dE galaxies would be one step further in the harassment scene. They would be bright spirals that have fully lost their disks. If this model is valid, and assuming that the central part of the objects do not change by harassment, then the structural parameters of dEs and the bulges of dS0s should be similar to the structural parameters of the bulges of bright spiral galaxies. Figure 14 shows the structural parameters of the dE galaxies and bulges of dS0, late-type, early-type and S0 galaxies in Coma. Table 4 shows the mean structural parameters of these types of galaxies. It can be seen that the scale of the inner parts of dS0 galaxies is similar to the bulges of late-type spirals, while dE galaxies show a larger scale. This result is similar if we consider only the more reliable sample of dS0 galaxies. This result indicates that dS0s are compatible with having been harassed late-type galaxies. But this is not so clear for dEs. It can be seen in Fig. 14 that the effective radii of the dE galaxies are in general larger than those of bulges of bright spirals. Nevertheless, some of them have similar scales to those of the bulges of early-type or S0 bright galaxies. We have found that 60% of dE galaxies are located at a distance of more than 3σ from the linear relation $r_e - M_R$ defined by the bulges of the bright spiral galaxies. These objects are not compatible with being harassed bright spiral galaxies.

Mastropietro et al. (2004) have found that late-type galaxies can evolve towards dE/dS0 systems by harassment. They conclude that late-type galaxies do not completely lose their disk with this mechanism. This would be in agreement with our evolutionary picture in which dS0 galaxies are harassed late-type spirals that have not fully lost the disk component. Mastropietro et al. (2004) have fitted the surface brightness profiles of their simulated dwarf galaxies with a single Sersic law. But in some cases the pure Sersic profile cannot fit the outermost points of the profile properly. These galaxies (Gal1, Gal5 and Gal7 from Mastropietro et al.) show important rotation features. This is similar what we observed in the surface brightness profiles of the dwarf galaxies in Coma. If, then, our dS0 galaxies are harassed bright spirals we can expect them to have a significant amount of rotation, similar to the simulated galaxies.

6. Conclusions

We have obtained the structural parameters of the dwarf galaxies in the Coma cluster with $-16 \leq M_B \leq -18$. The galaxies were classified into two types according to the fit of their surface brightness profiles. Those objects fitted with one component (Sersic profile) were called dE galaxies (56%), and those fitted with two components (Sersic and exponential profiles) were called dS0s (29%). The other 15% correspond to objects for which no reliable photometry could be obtained owing to the presence of bright nearby objects.

The structural parameters of dE and dS0 galaxies in Coma are similar to those shown by the same kinds of objects in the Virgo cluster. There is a smooth and continuous relation between the structural parameters of dEs and bright E galaxies in the Coma cluster. On the other hand, the structural parameters of the exponential profiles of dS0 galaxies are also related with those from the disks of bright spiral galaxies in the Coma cluster.

The typical global scales of dE and dS0 galaxies in Coma are similar, although dS0 galaxies are flatter than dEs. The differences in color, mean velocity, and velocity dispersion between the different groups of galaxies are not statistically significant. The scale of the bulges of late-type Coma galaxies is similar to the scale of the bulges of dS0 galaxies. Nevertheless, the mean scale of dEs is larger than that of the bulges of all groups of bright galaxies.

Assuming the picture in which dwarf galaxies come from harassed bright disk ones, we conclude that dS0 galaxies are harassed late-type spirals that have lost much of their disks. On the contrary, most of the dE galaxies (60%) do not fit well in this evolutionary model, and other physical mechanisms are required for their genesis.

We would like to thank to B. M. Poggianti and C. Mastropietro for useful discussions in the preparation of this manuscript. We wish also to thank to the anonymous referee for useful comments, which have improved the quality of this paper. This research has made use of the Isaac Newton Telescope operated by the Isaac Newton group on La Palma at the Spanish del Roque de los Muchachos Observatory of the Instituto de Astrofísica de Canarias. The authors were founded by the Spanish DGES, grant AYA2001-3939.

REFERENCES

- Aguerri, J. A. L., Iglesias-Paramo, J., Vilchez, J. M., & Muñoz-Tuñón, C. 2004, AJ, 127, 1344
- Aguerri, J. A. L. & Trujillo, I. 2002, MNRAS, 333, 633
- Aguerri, J. A. L., Balcells, M., & Peletier, R. F. 2001, A&A, 367, 428
- Andreon, S., Davoust, E., & Poulain, P. 1997, A&AS, 126, 67
- Andreon, S., Davoust, E., Michard, R., Nieto, J.-L., & Poulain, P. 1996, A&AS, 116, 429
- Barazza, F. D., Binggeli, B., & Jerjen, H. 2003, A&A, 407, 121
- Barazza, F. D., Binggeli, B., & Jerjen, H. 2002, A&A, 391, 823
- Beers, T. C., Flynn, K., & Gebhardt, K. 1990, AJ, 100, 32
- Bekki, K., Couch, W. J., & Shioya, Y. 2002, ApJ, 577, 651
- Bekki, K. 2001, ApJ, 546, 189
- Bertin, E. & Arnouts, S. 1996, A&AS, 117, 393
- Binggeli, B. & Popescu, C. C. 1995, A&A, 298, 63
- Binggeli, B. & Cameron, L. M. 1991, A&A, 252, 27
- Binggeli, B., Sandage, A., & Tammann, G. A. 1988, ARA&A, 26, 509
- Binggeli, B., Sandage, A., & Tammann, G. A. 1985, AJ, 90, 1681
- Biviano, A. & Katgert, P. 2004, A&A, 424, 779
- Caldwell, N. & Bothun, G. D. 1987, AJ, 94, 1126

- Caon, N., Capaccioli, M., & D’Onofrio, M. 1993, MNRAS, 265, 1013
- de Blok, W. J. G., van der Hulst, J. M., & Bothun, G. D. 1995, MNRAS, 274, 235
- Dekel, A. & Silk, J. 1986, ApJ, 303, 39
- De Young, D. S. & Gallagher, J. S. 1990, ApJ, 356, L15
- Driver, S. P., Phillipps, S., Davies, J. I., Morgan, I., & Disney, M. J. 1994, MNRAS, 266, 155
- Durrell, P. R. 1997, AJ, 113, 531
- Freeman, K. C. 1970, ApJ, 160, 811
- Geha, M., Guhathakurta, P., & van der Marel, R. P. 2003, AJ, 126, 1794
- Godwin, J. G., Metcalfe, N., & Peach, J. V. 1983, MNRAS, 202, 113
- Graham, A. W. & Guzmán, R. 2003, AJ, 125, 2936
- Gunn, J. E. & Gott, J. R. I. 1972, ApJ, 176, 1
- Gutiérrez, C. M., Trujillo, I., Aguerri, J. A. L., Graham, A. W., & Caon, N. 2004, ApJ, 602, 664
- Iglesias-Páramo, J., Boselli, A., Gavazzi, G., Cortese, L., & Vílchez, J. M. 2003, A&A, 397, 421
- Iglesias-Páramo, J., Boselli, A., Cortese, L., Vílchez, J. M., & Gavazzi, G. 2002, A&A, 384, 383
- Jerjen, H., Kalnajs, A., & Binggeli, B. 2000, A&A, 358, 845
- Jerjen, H. & Binggeli, B. 1997, ASP Conf. Ser. 116: The Nature of Elliptical Galaxies; 2nd Stromlo Symposium, 239
- Kormendy, J. 1985, ApJ, 295, 73
- Lin, D. N. C. & Faber, S. M. 1983, ApJ, 266, L21
- Mastropietro, C., Moore, B., Mayer, L., Debattista, V. P., Piffaretti, R., & Stadel, J. 2004, astro-ph/0411648
- Mayer, L., Governato, F., Colpi, M., Moore, B., Quinn, T., Wadsley, J., Stadel, J., & Lake, G. 2001a, ApJ, 559, 754

- Mayer, L., Governato, F., Colpi, M., Moore, B., Quinn, T., Wadsley, J., Stadel, J., & Lake, G. 2001b, *ApJ*, 547, L123
- Mobasher, B., et al. 2003, *ApJ*, 587, 605
- Moore, B., Gelato, S., Jenkins, A., Pearce, F. R., & Quilis, V. 2000, *ApJ*, 535, L21
- Moore, B., Lake, G., Quinn, T., & Stadel, J. 1999, *MNRAS*, 304, 465
- Moore, B., Lake, G., & Katz, N. 1998, *ApJ*, 495, 139
- Moore, B., Katz, N., Lake, G., Dressler, A., & Oemler, A. 1996, *Nature*, 379, 613
- Navarro, J. F., Frenk, C. S., & White, S. D. M. 1997, *ApJ*, 490, 493
- Patterson, R. J. & Thuan, T. X. 1996, *ApJS*, 107, 103
- Pedraz, S., Gorgas, J., Cardiel, N., Sánchez-Blázquez, P., & Guzmán, R. 2002, *MNRAS*, 332, L59
- Phillipps, S., Driver, S. P., Couch, W. J., & Smith, R. M. 1998, *ApJ*, 498, L119
- Poggianti, B. M., et al. 2001, *ApJ*, 562, 689
- Pracy, M. B., De Propris, R., Driver, S. P., Couch, W. J., & Nulsen, P. E. J. 2004, *MNRAS*, 352, 1135
- Quilis, V., Moore, B., & Bower, R. 2000, *Science*, 288, 1617
- Richer, M. G. & McCall, M. L. 1995, *ApJ*, 445, 642
- Ryden, B. S., Terndrup, D. M., Pogge, R. W., & Lauer, T. R. 1999, *ApJ*, 517, 650
- Sánchez-Janssen, R., Iglesias-Páramo, J., Muñoz-Tuñón, C., Aguerri, J. A. L. & Vilchez, J. M. 2005, *A&A*, in press
- Sandage, A. & Binggeli, B. 1984, *AJ*, 89, 919
- Secker, J., Harris, W. E., & Plummer, J. D. 1997, *PASP*, 109, 1377
- Sersic, J. L. 1968, *Atlas de Galaxies Australes*; Vol. Book; Page 1, 0
- Silich, S. & Tenorio-Tagle, G. 2001, *ApJ*, 552, 91
- Skillman, E. D., Kennicutt, R. C., & Hodge, P. W. 1989, *ApJ*, 347, 875

- Thompson, L. A. & Gregory, S. A. 1993, AJ, 106, 2197
- Toomre, A. & Toomre, J. 1972, ApJ, 178, 623
- Trentham, N. 1998, MNRAS, 293, 71
- Trujillo, I. & Aguerri, J. A. L. 2004, MNRAS, 355, 82
- Trujillo, I., Aguerri, J. A. L., Gutiérrez, C. M., Caon, N., & Cepa, J. 2002, ApJ, 573, L9
- Trujillo, I., Aguerri, J. A. L., Gutiérrez, C. M., & Cepa, J. 2001a, AJ, 122, 38
- Trujillo, I., Aguerri, J. A. L., Cepa, J., & Gutiérrez, C. M. 2001b, MNRAS, 328, 977
- Trujillo, I., Aguerri, J. A. L., Cepa, J., & Gutiérrez, C. M. 2001c, MNRAS, 321, 269
- van Zee, L., Skillman, E. D., & Haynes, M. P. 2004a, AJ, 128, 121
- van Zee, L., Barton, E. J., & Skillman, E. D. 2004b, AJ, in press
- van Zee, L., Salzer, J. J., & Skillman, E. D. 2001, AJ, 122, 121
- van Zee, L. 2000, AJ, 119, 2757

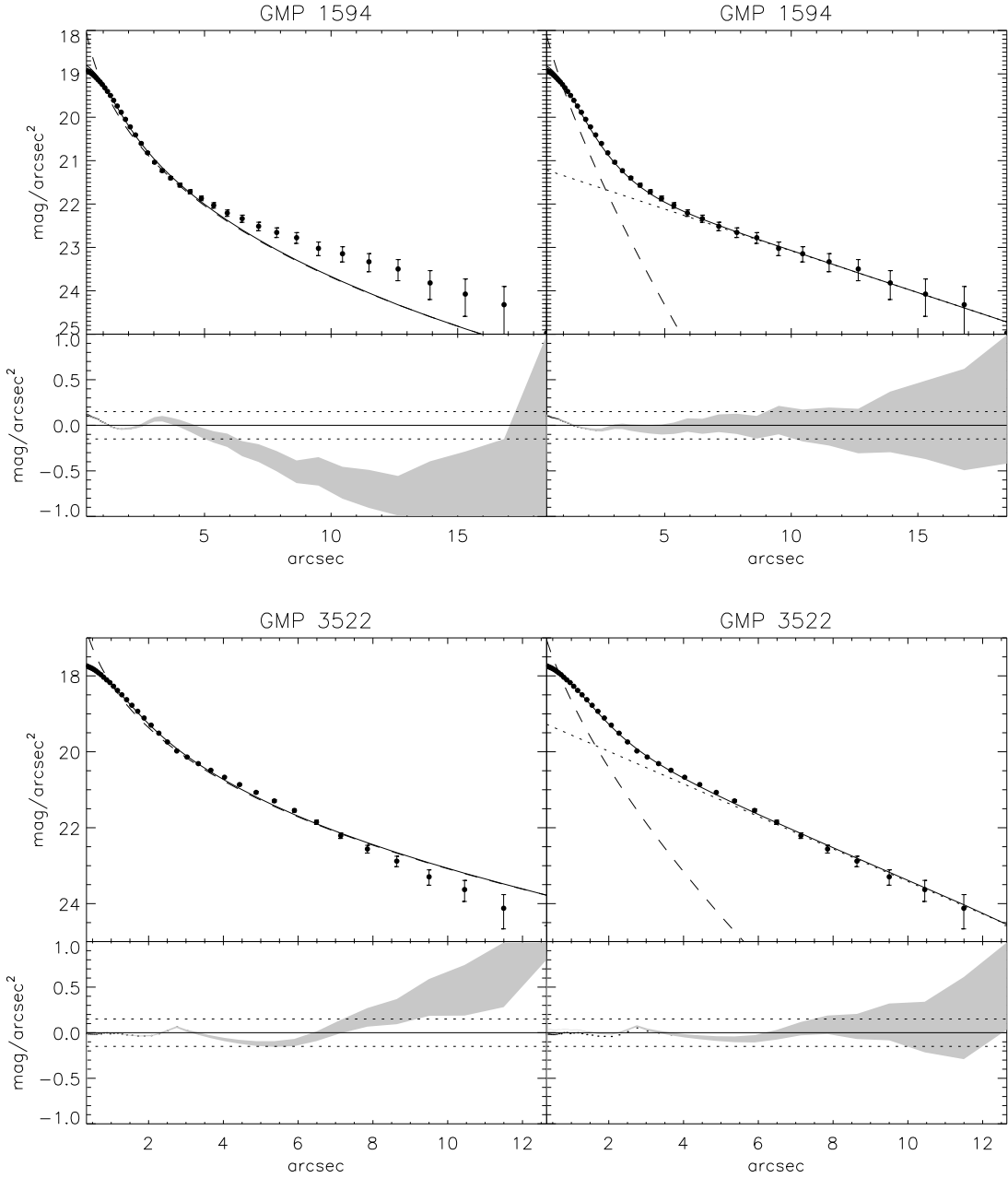


Fig. 1.— Surface brightness profiles of GMP 1594 and GMP 3522 fitted with one Sersic profile (left panels) and Sersic+exponential profiles (right panels). The dashed line represent the Sersic profile, the dotted line the exponential one. The full line represents the convolved total fitted model. Also shown are the residuals of each fit. The dotted horizontal lines represent residuals of $\pm 0.15 \text{ mag arcsec}^{-2}$.

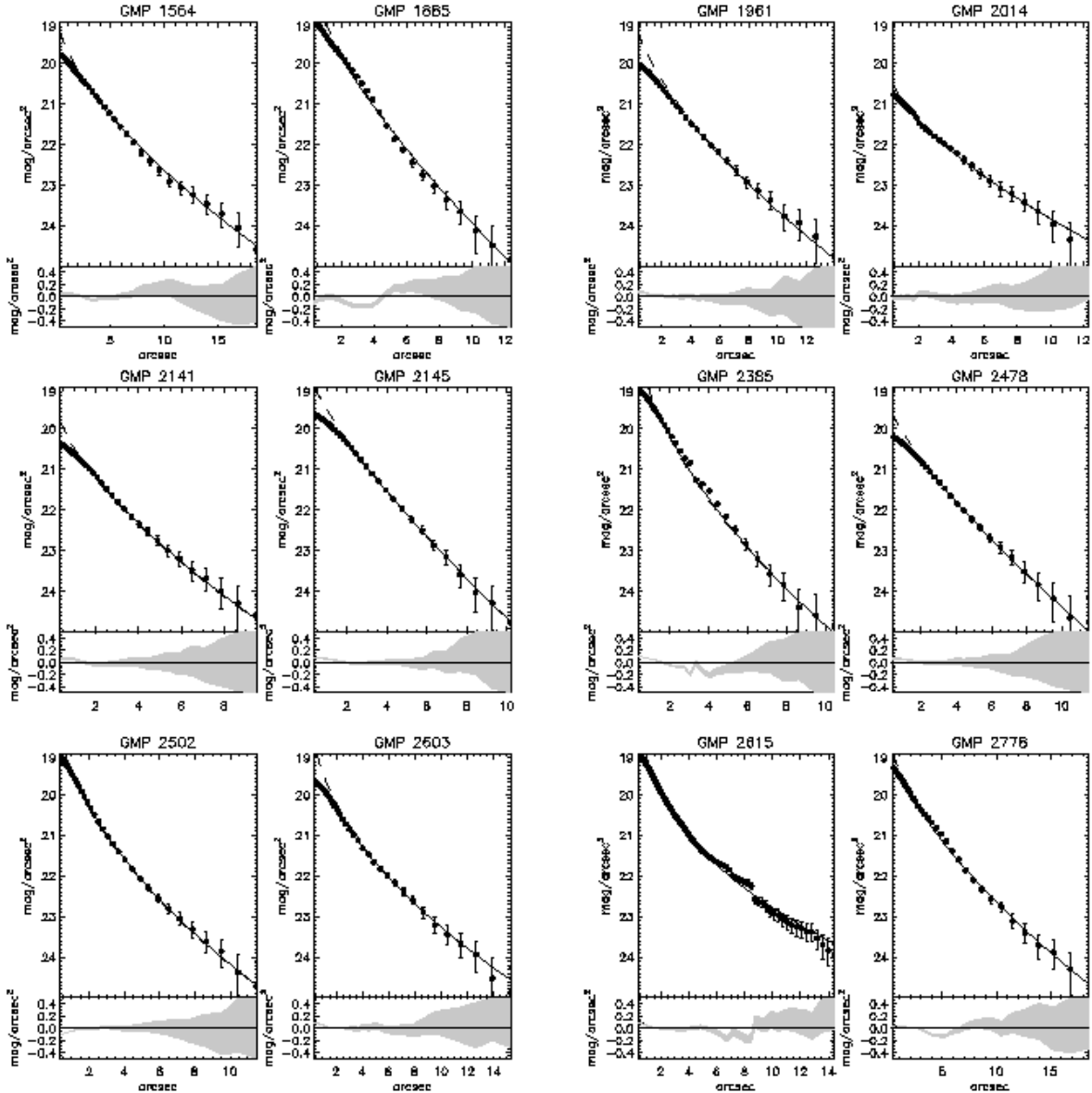


Fig. 2.— Surface brightness, ellipticity, and position angle isophotal profiles of the dE galaxies. Also overplotted is the Sersic profile fitted (dashed line) to the surface brightness profiles and the residuals. The full line represents the convolved Sersic fitted profile.

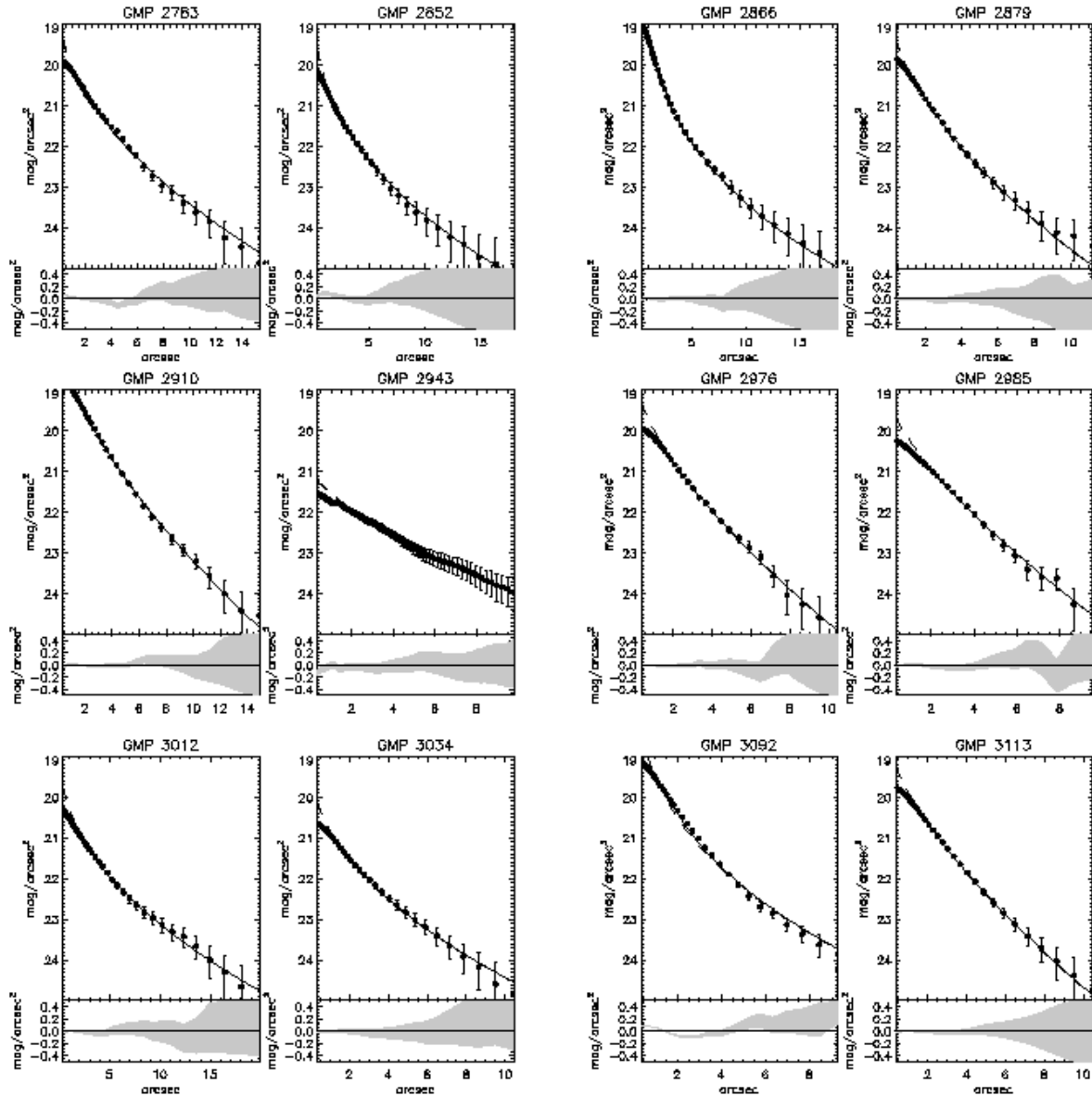


Fig. 2.— Continued

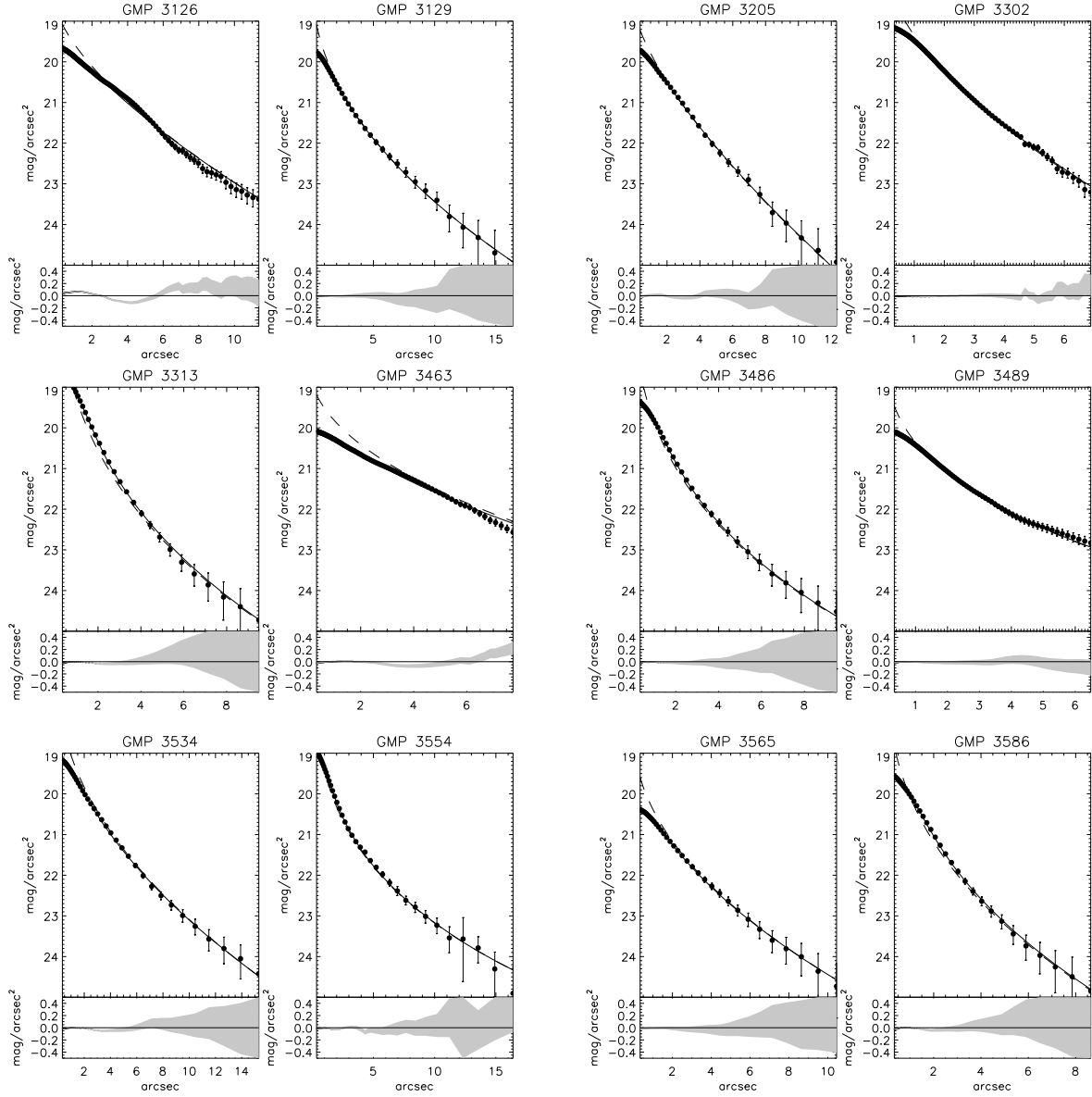


Fig. 2.— Continued

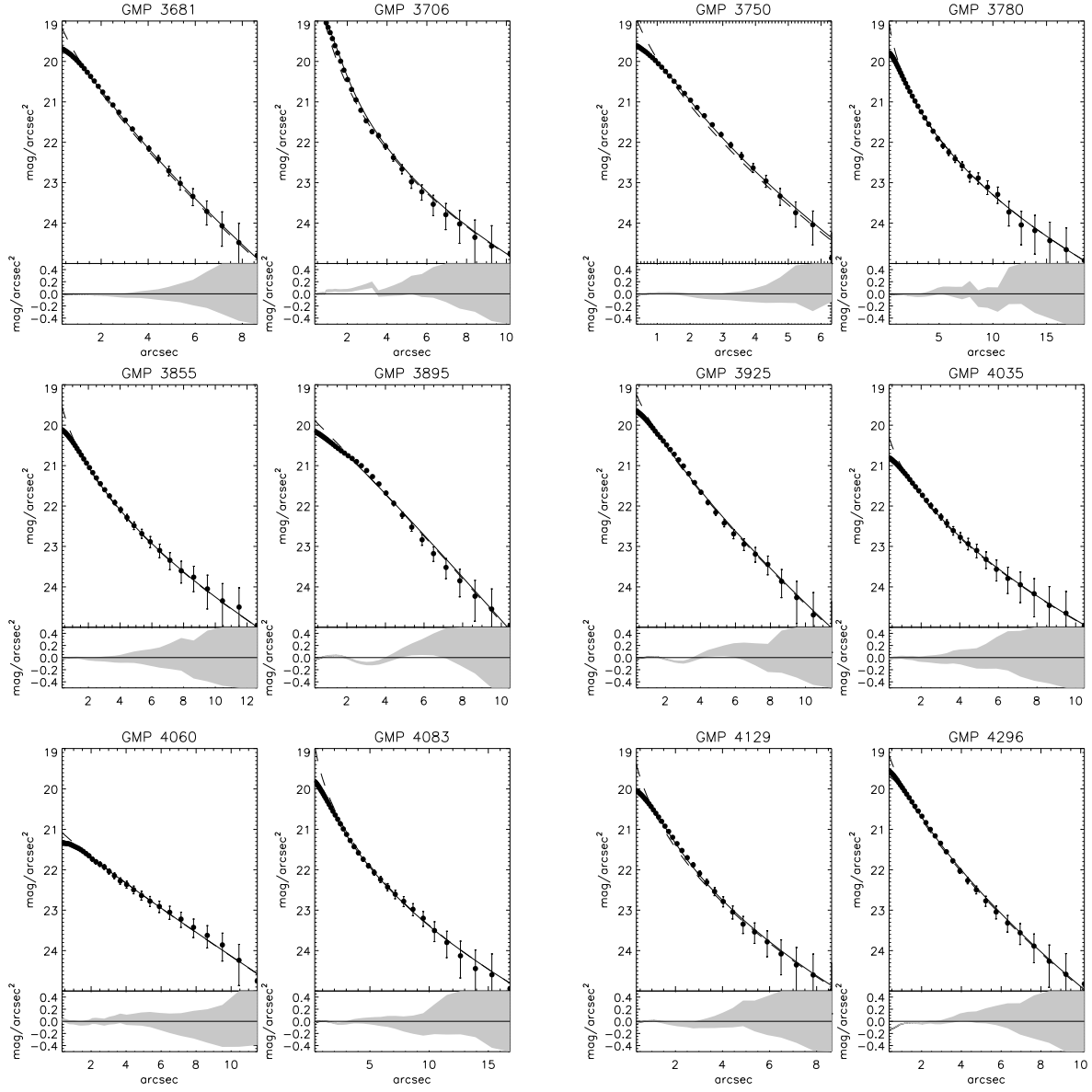


Fig. 2.— Continued

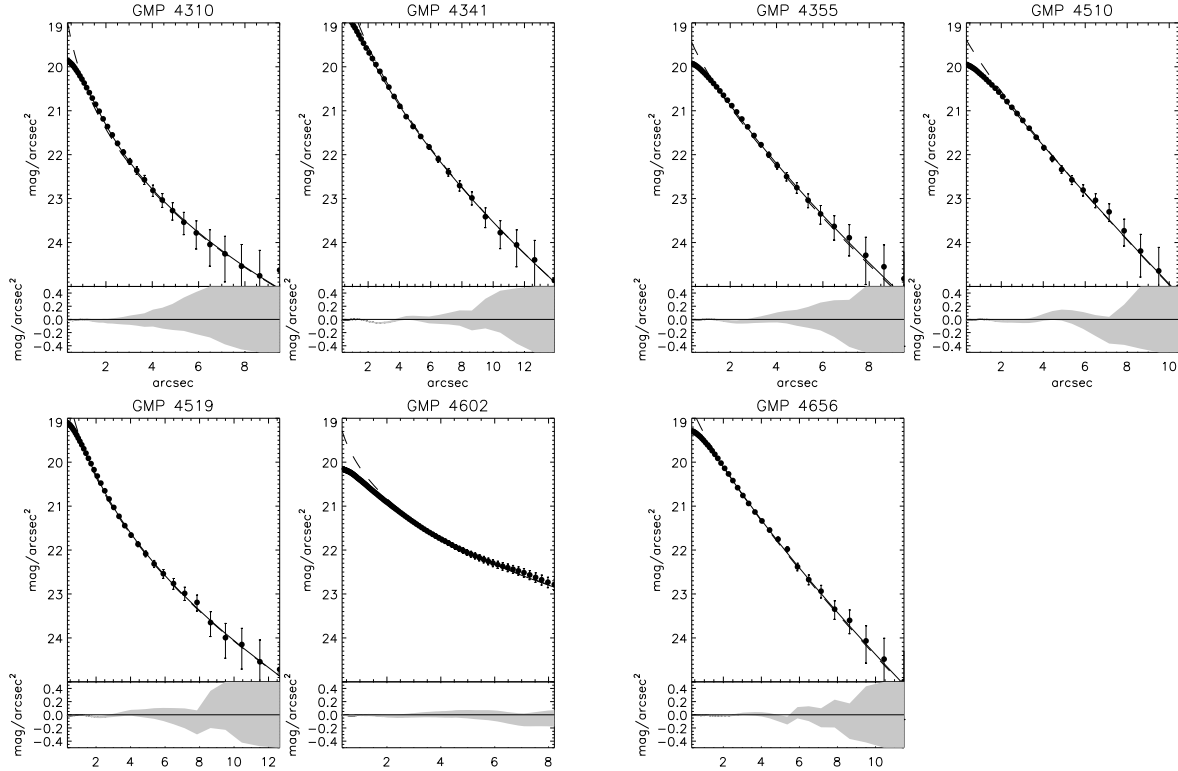


Fig. 2.— Continued

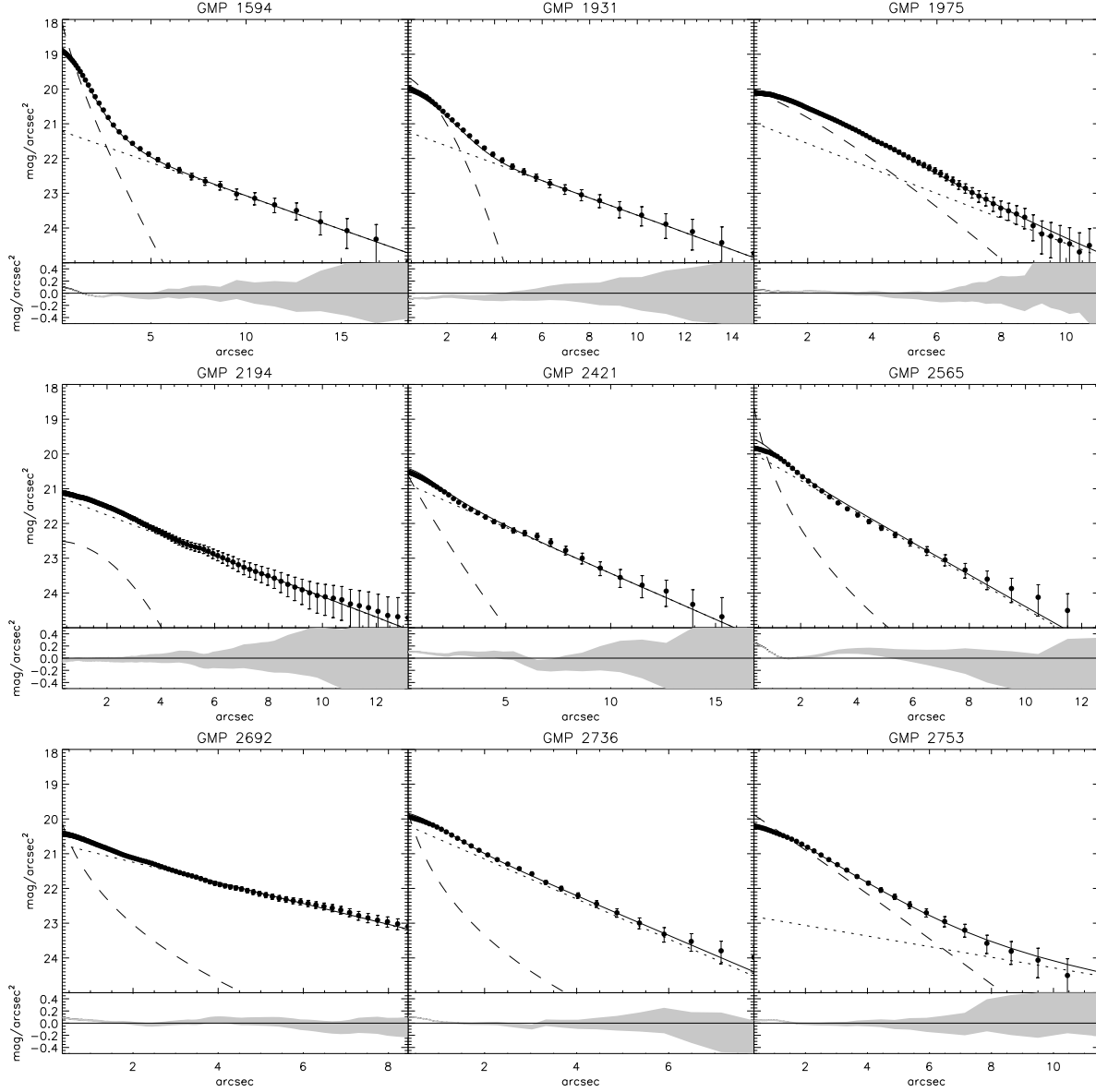


Fig. 3.— Surface brightness, ellipticity, and position angle isophotal profiles of the dS0 galaxies. Also overplotted is the Sersic (dashed line) and exponential (dotted line) profiles fitted to the surface brightness profiles and the residuals. The full line represents the total convolved fitted profile.

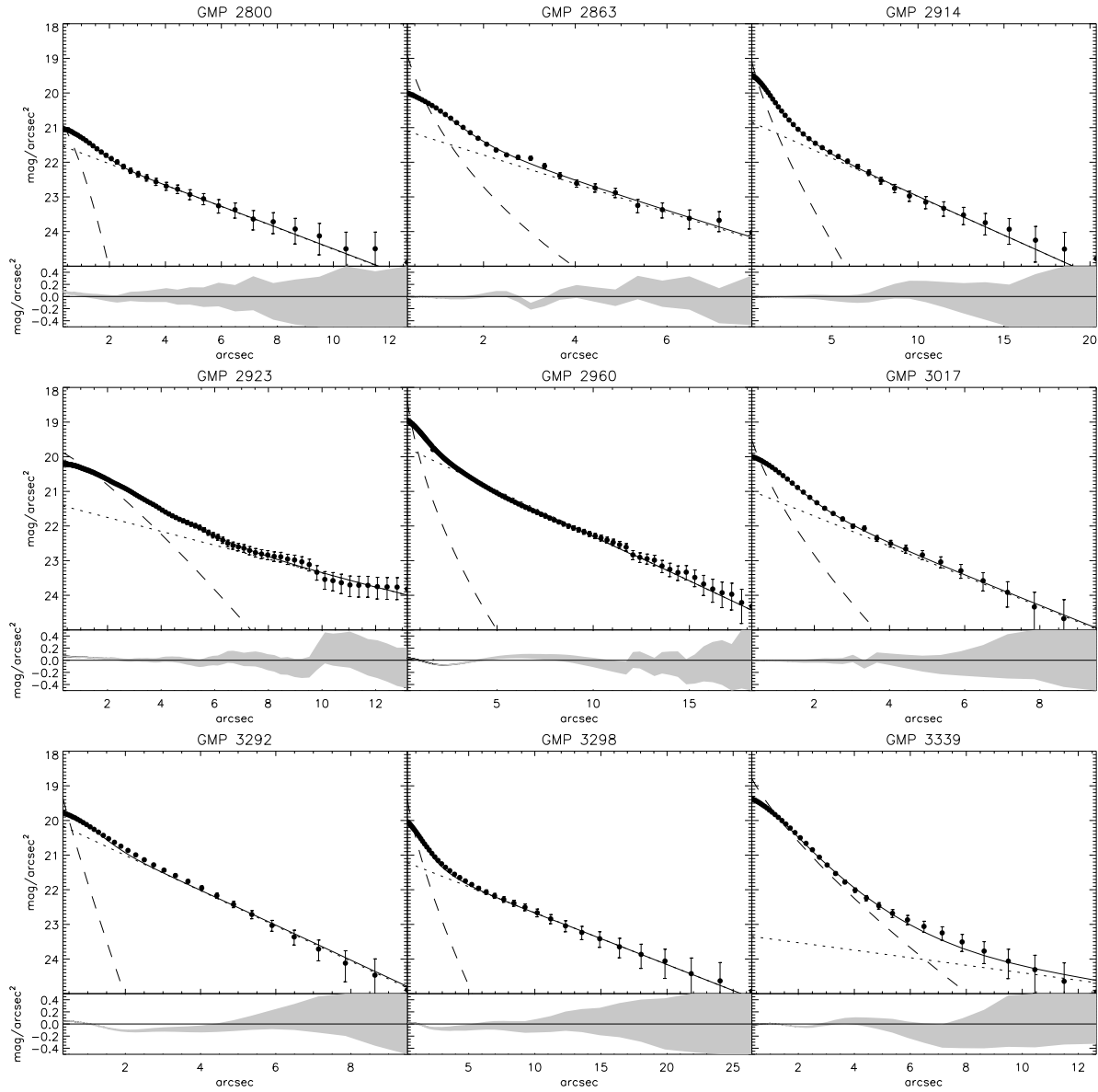


Fig. 3.— Continued

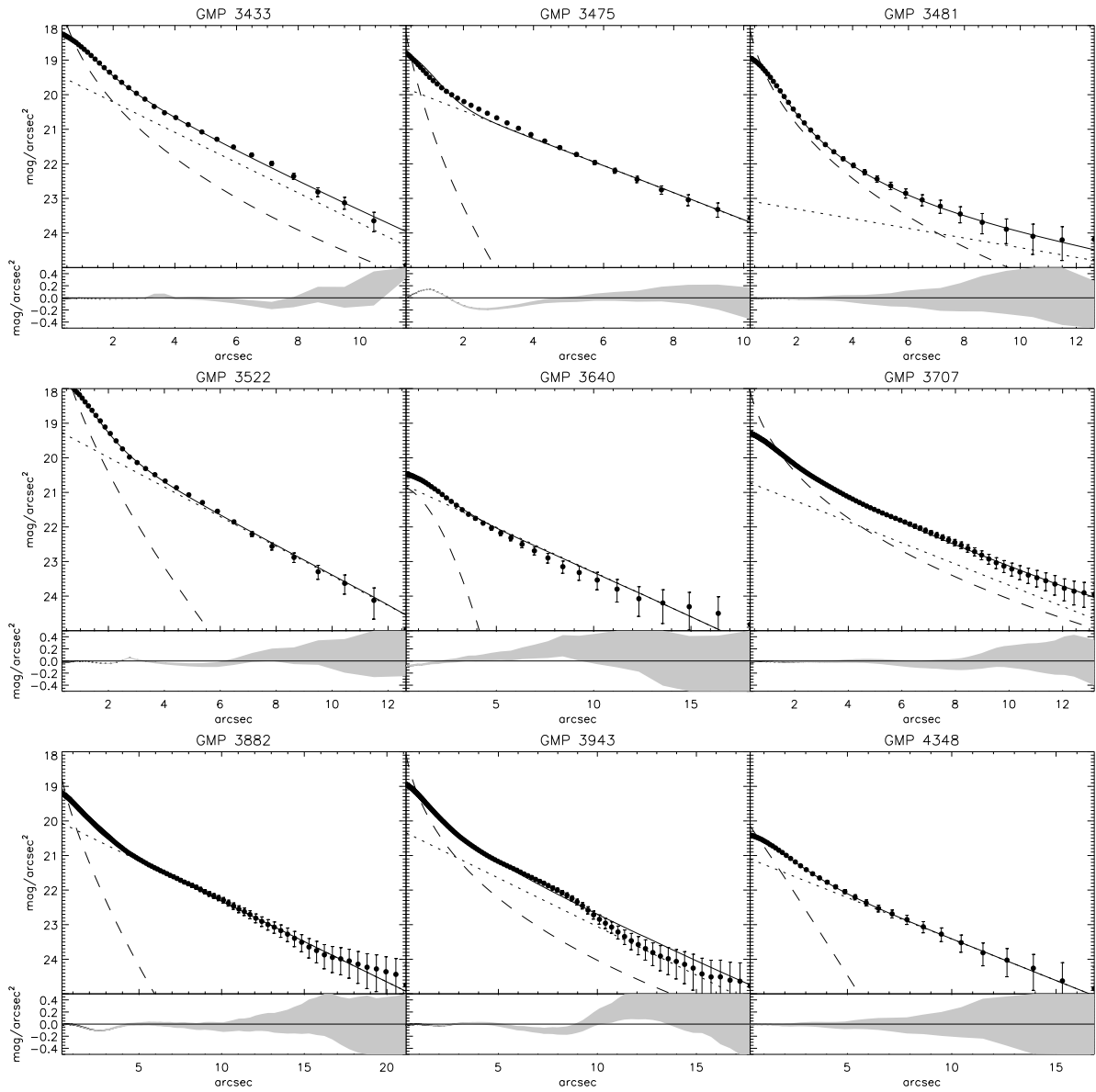


Fig. 3.— Continued

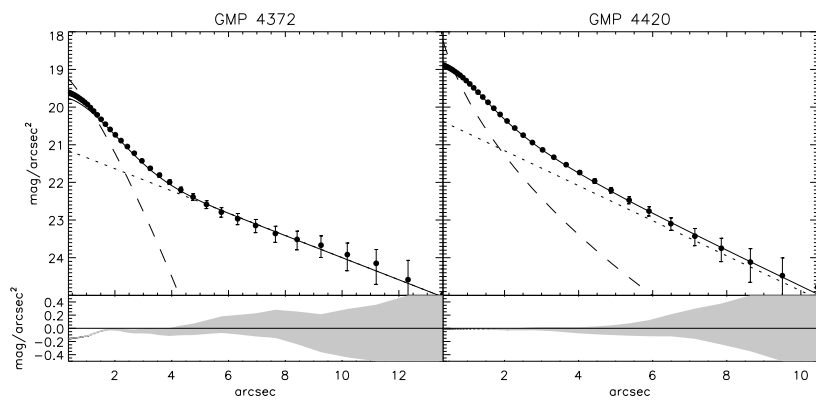


Fig. 3.— Continued

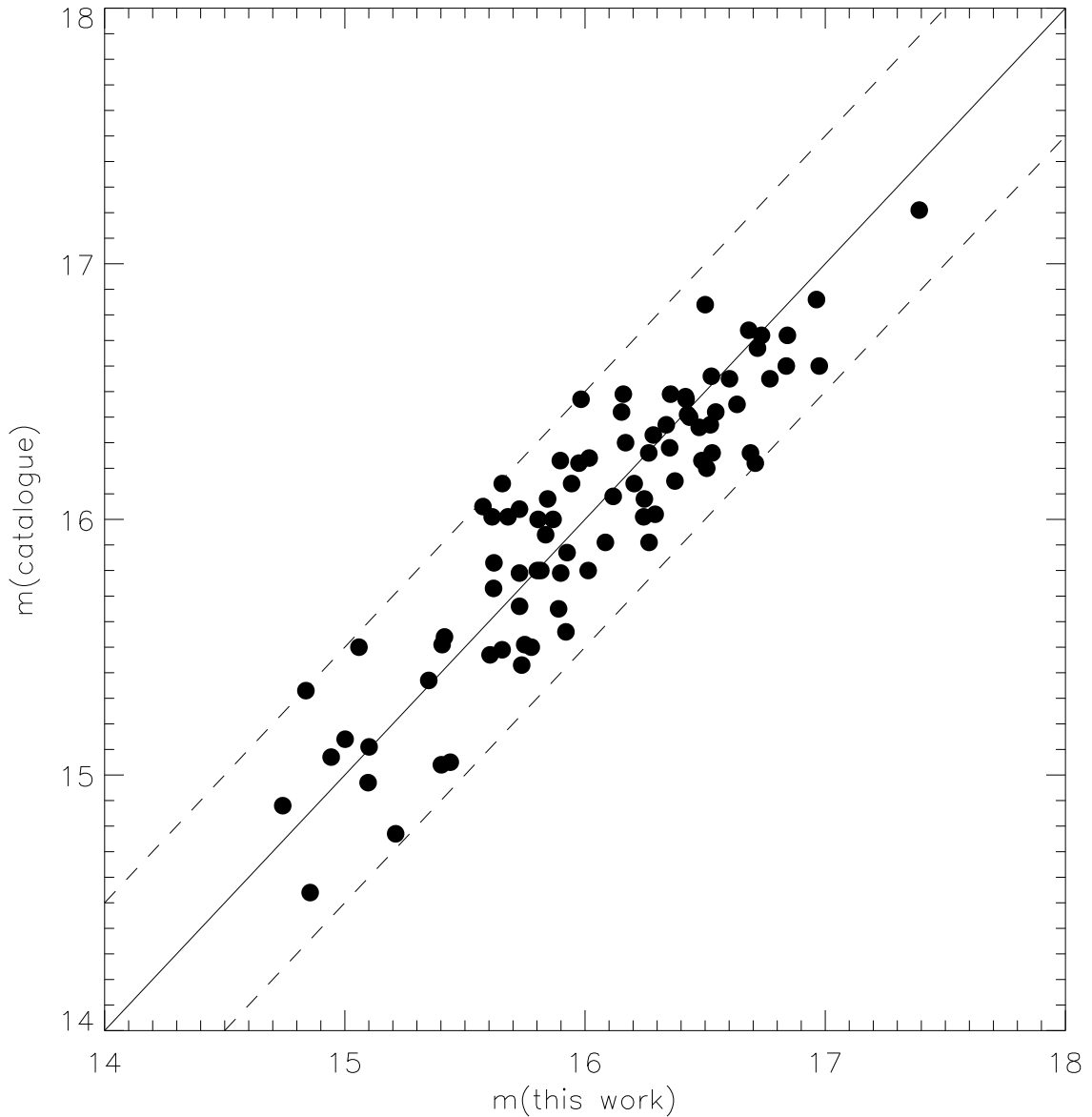


Fig. 4.— Comparison of the magnitudes of the objects from Godwin et al. (1983) and those obtained from our model fits. The dashed lines represents a deviation of 0.5 magnitudes.

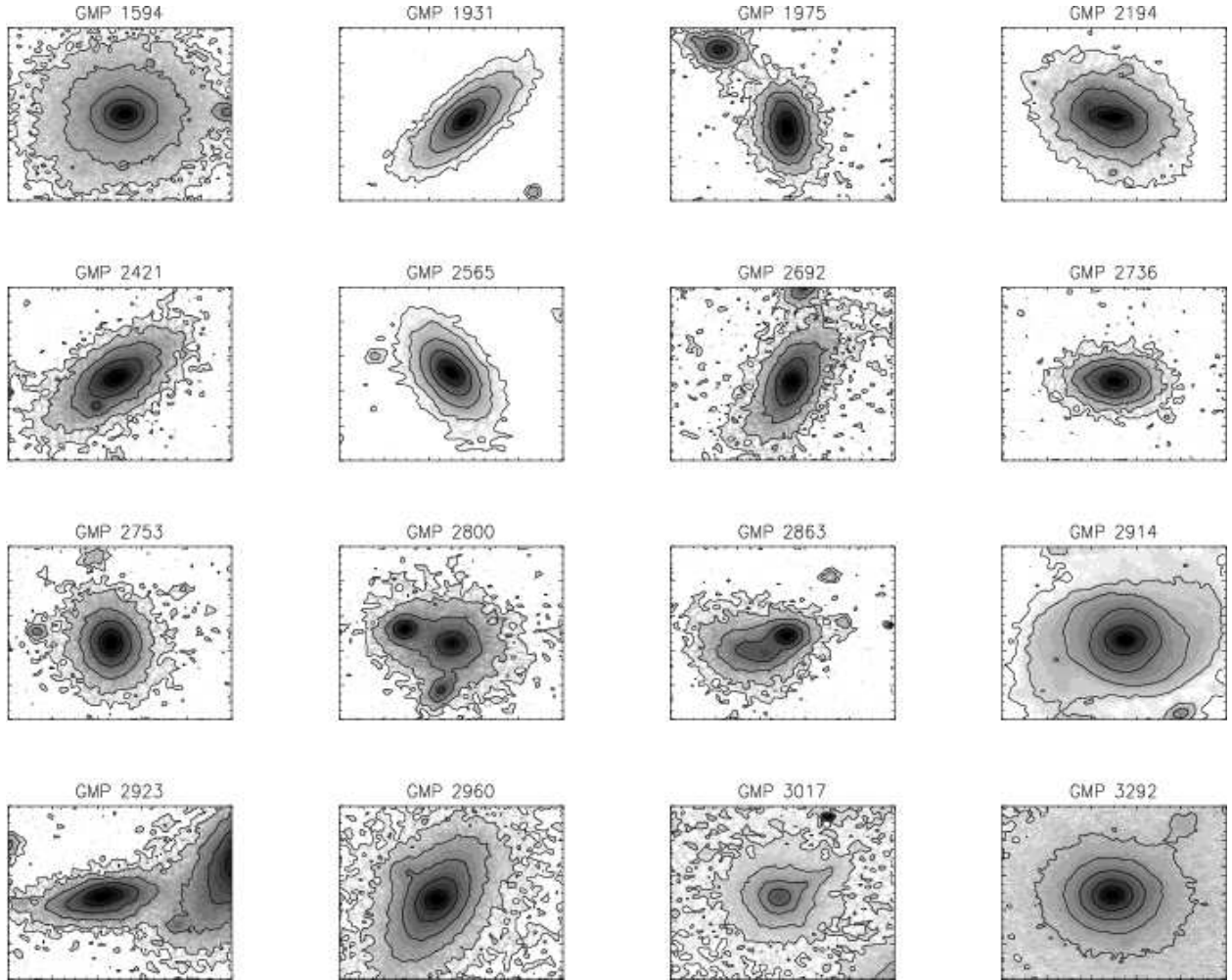


Fig. 5.— R-band images of the dS0 galaxies. The isocontours are spaced at 1 mag/arcsec², and the outermost corresponds to $\mu_r = 25$ mag/arcsec². The size of each panel is 33 arcsec.

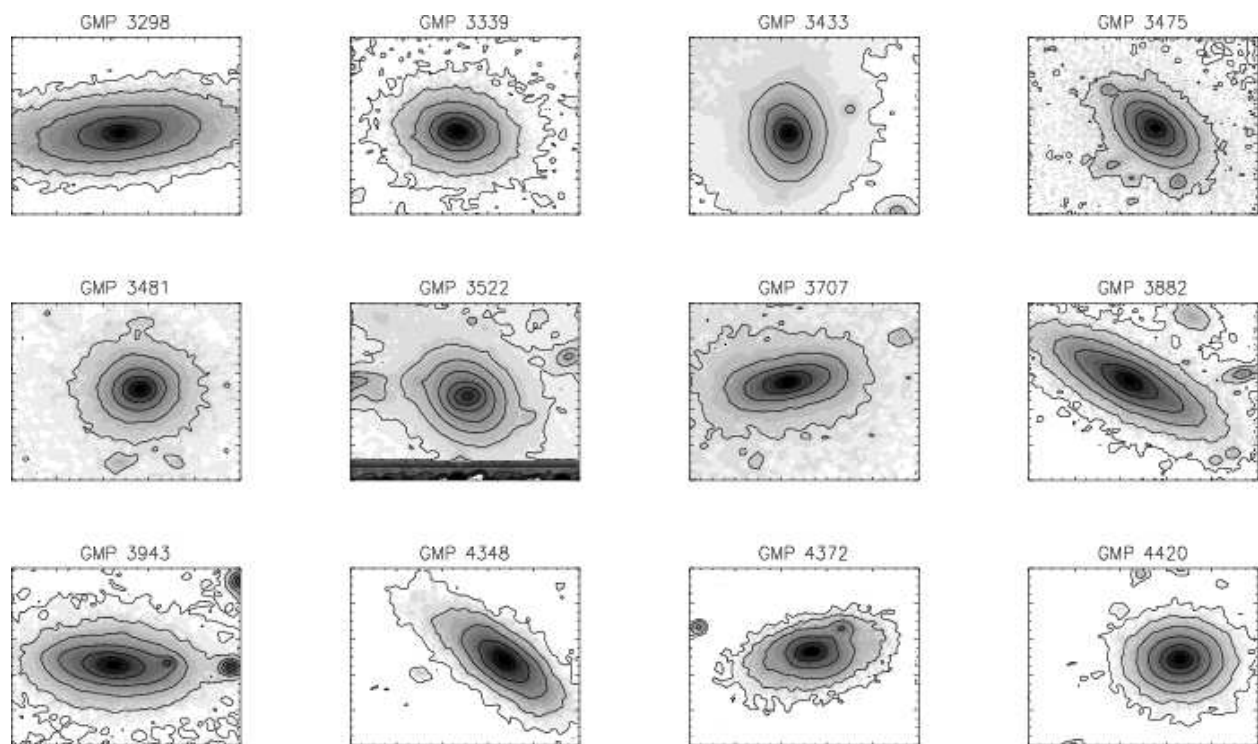


Fig. 5.— Continued

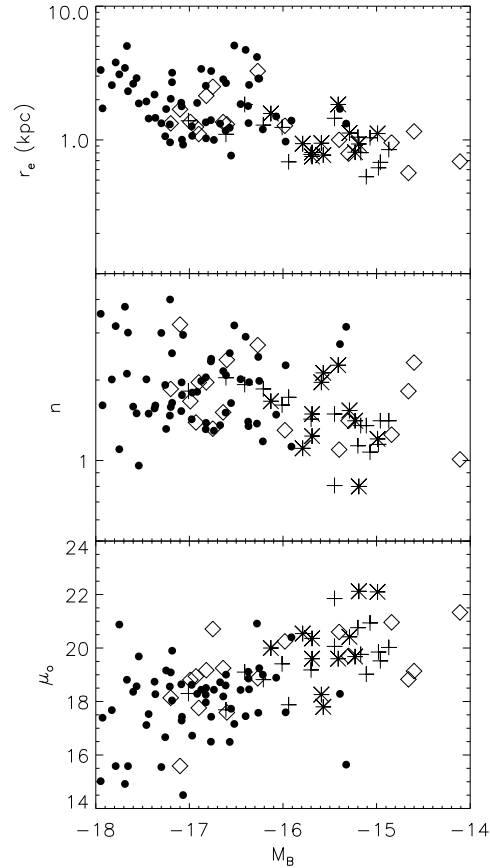


Fig. 6.— Effective radius (top panel), shape parameter (middle panel) and central surface brightness (bottom panel) as a function of the absolute B magnitudes of dE galaxies in the Coma (full points) and Virgo clusters. The data for the Virgo cluster are from Barazza et al. (2003) (diamonds); Durrell (1997) (crosses), and van Zee et al. (2004) (asterisks).

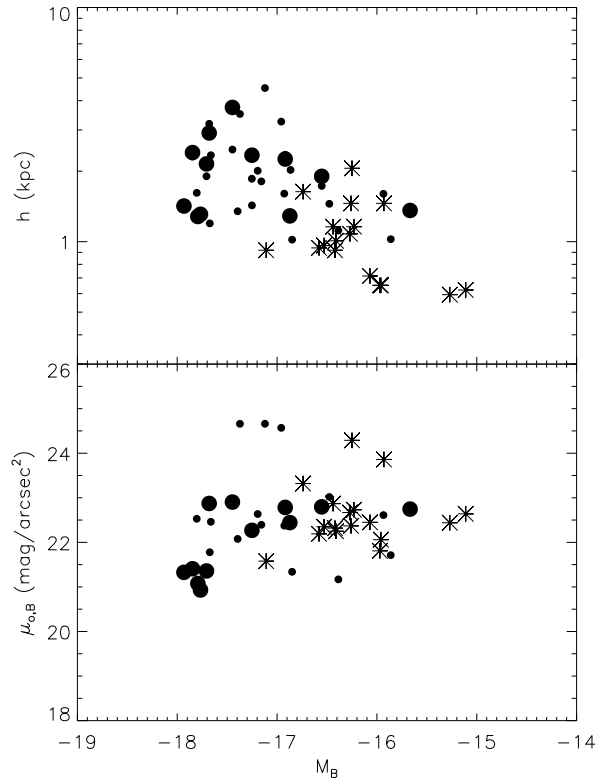


Fig. 7.— Scale-length (top panel) and central surface brightness (bottom panel) of the exponential component as function of the absolute B -band magnitudes for the dS0 galaxies in the Coma (filled circles) and Virgo (asterisks). The large filled circles represent the dS0 Coma galaxies from the more reliable sample (see text for more details).

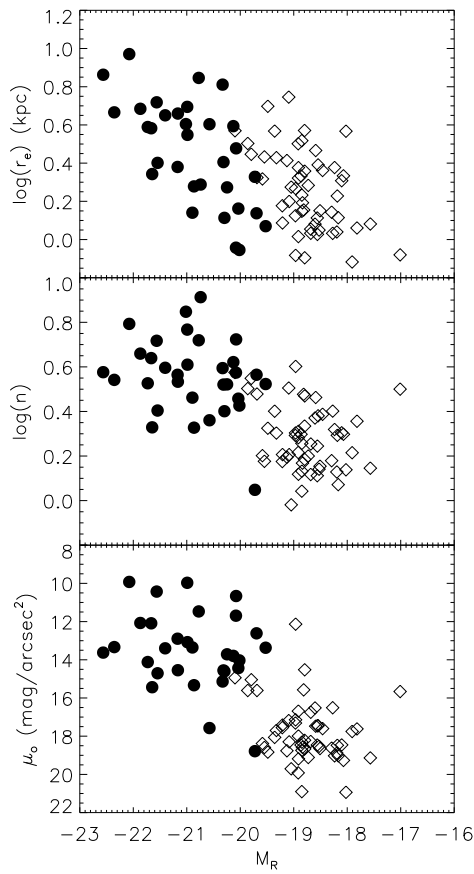


Fig. 8.— Scale length (top panel), Sersic shape parameter (middle panel), and central surface brightness (bottom panel) as a function of the R -band absolute magnitude magnitudes of Bright E (full points) and dE (diamonds) galaxies in the Coma cluster.

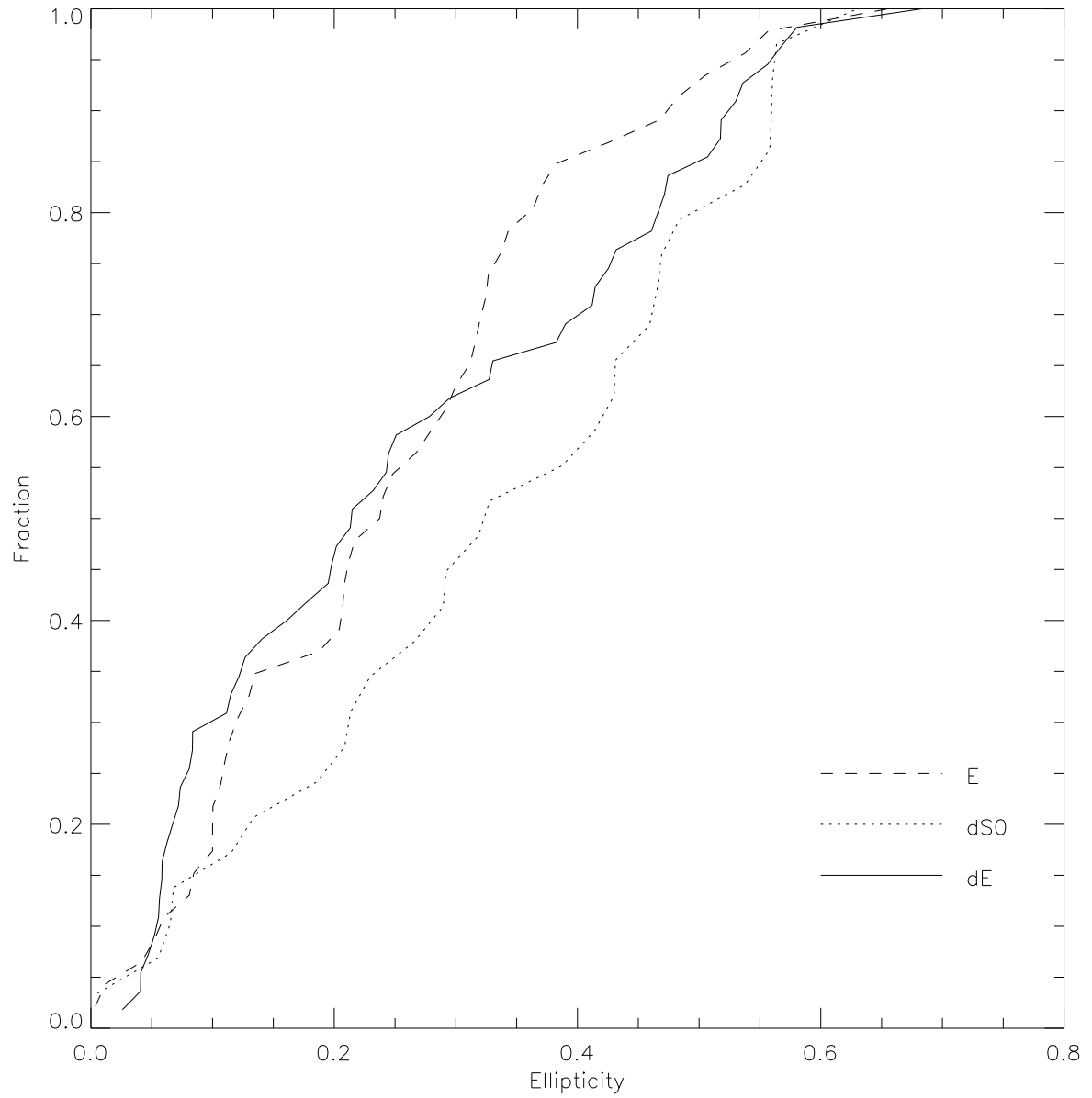


Fig. 9.— Cumulative distribution function of the ellipticity of E (dashed line), dE (full line), and dS0 (dotted line) galaxies.

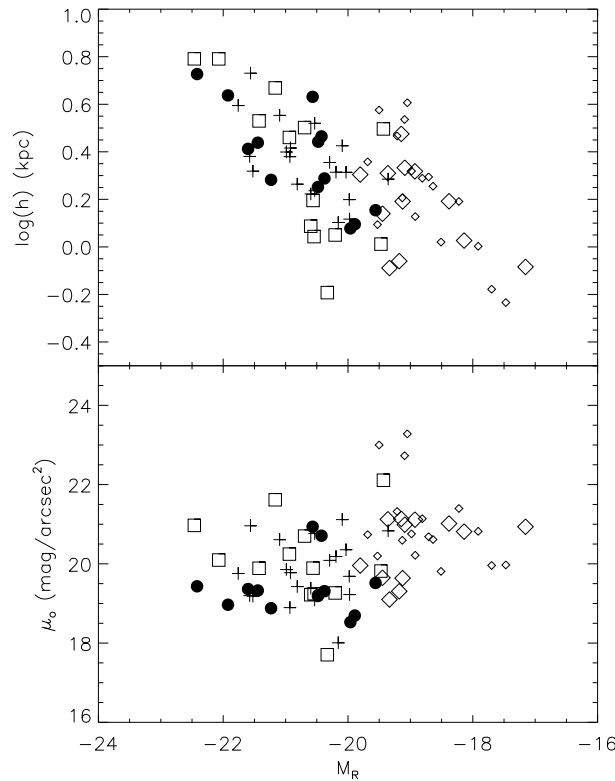


Fig. 10.— Scale length (top panel) and central surface brightness (bottom panels) as a function of the absolute R -band magnitudes of the galaxies for the disk component of dS0 and bright spirals in the Coma cluster. The symbols represent dS0 (diamonds), late type spirals (full points), early type spirals (crosses) and bright S0 (squares) galaxies. The large diamonds represent the more reliable sample of dS0 galaxies.

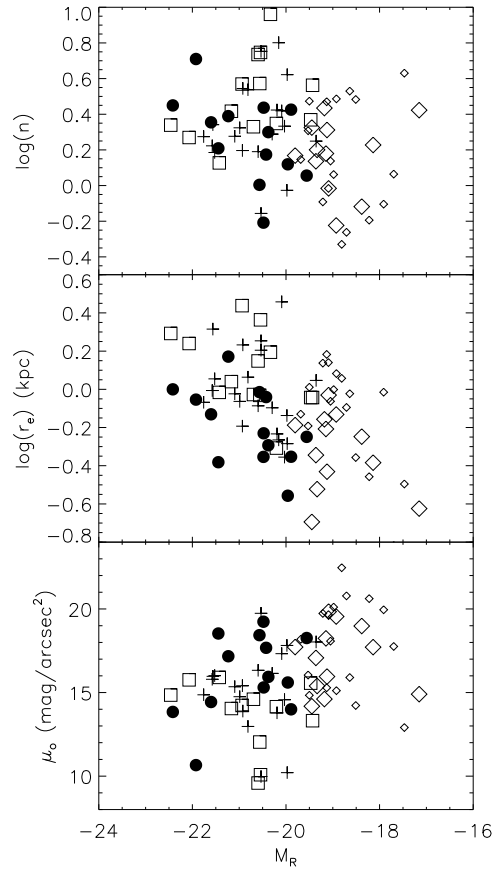


Fig. 11.— Sersic shape parameter, n (top panel), effective radius (middle panel), and central surface brightness (bottom panel) as a function of the absolute magnitude of the galaxies for the bulges of dS0 and bright spirals in Coma. Symbols are as in Figure 10.

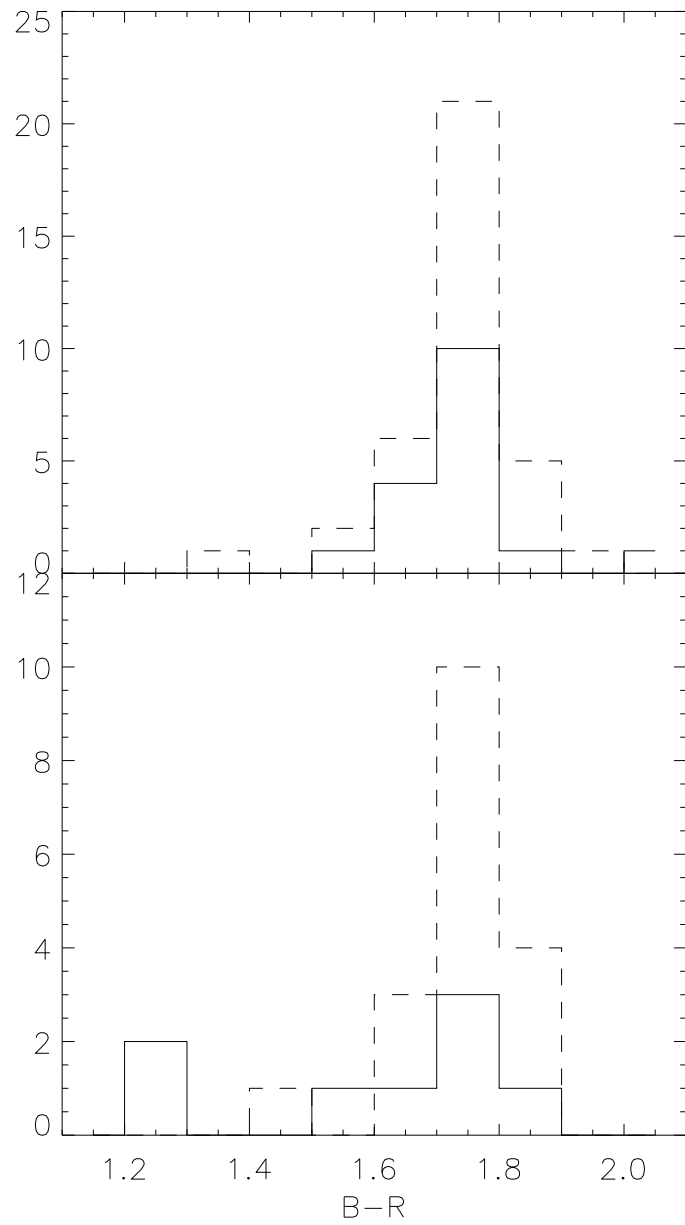


Fig. 12.— $B-R$ color distribution of dS0 (dashed lines) and dE (solid lines) galaxies located at $R/r_s < 2$ (top panel) and $R/r_s > 2$ (bottom panel).

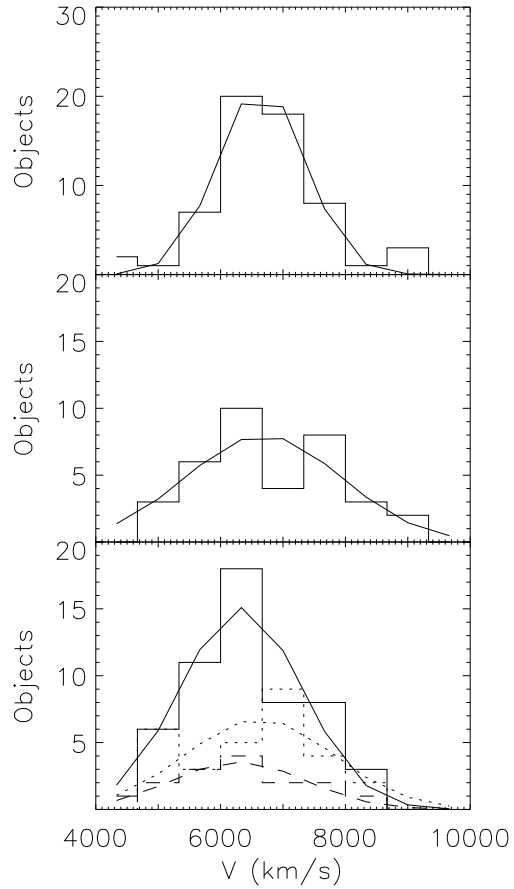


Fig. 13.— Histograms of the line of sight velocities of ellipticals (top panel), bright spirals (middle panel), and dwarfs (bottom panel). In the bottom panel the full lines represent dEs, the dotted lines show dS0s, and the dashed lines correspond to the more reliable sample of dS0s. The Gaussian fits of the different velocity distributions are also overplotted.

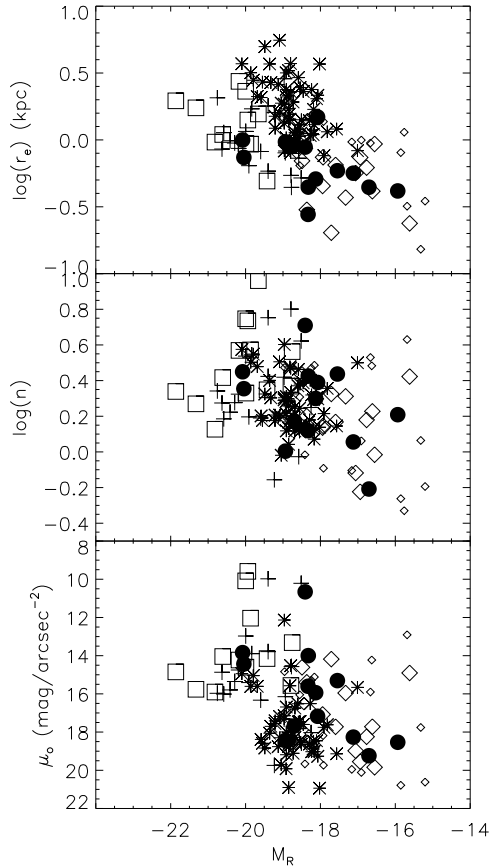


Fig. 14.— Effective radius (top panel), Sersic shape parameter, n (middle panel), and central surface brightness (bottom panel) as a function of the absolute magnitude of the dE galaxies (asterisks) and bulges of dS0 (diamonds), late-type (full points), early-type (crosses) and S0 (squares) galaxies in Coma.

Table 1. Structural parameters of the dE galaxies

| GMP (1) | V_{\odot} (2) | M_B (3) | M_R (4) | μ_e (5) | r_e (6) | n (7) | ϵ (8) |
|------------|--------------------|--------------|--------------|----------------|--------------|------------|-------------------|
| 1564 | 5937 | -17.41 | -19.13 | 21.81 | 6.91 | 1.57 | 0.47 |
| 1885 | 7802 | -17.49 | -19.21 | 20.45 | 3.07 | 1.50 | 0.52 |
| 1961 | 7915 | -17.14 | -18.80 | 21.63 | 4.59 | 1.53 | 0.58 |
| 2014 | 6885 | -17.23 | -18.92 | 23.13 | 7.31 | 1.64 | 0.05 |
| 2141 | 8220 | -17.25 | -18.73 | 22.20 | 3.73 | 1.59 | 0.08 |
| 2145 | 6834 | -16.78 | -18.56 | 20.91 | 3.01 | 1.29 | 0.41 |
| 2385 | 7092 | -17.31 | -18.91 | 20.49 | 2.32 | 1.92 | 0.28 |
| 2478 | 8765 | -17.31 | -18.91 | 21.68 | 3.82 | 1.31 | 0.39 |
| 2502 | 6392 | -17.13 | -18.97 | 21.21 | 3.30 | 1.96 | 0.11 |
| 2603 | 8181 | -17.88 | -19.32 | 21.71 | 5.23 | 2.01 | 0.54 |
| 2615 | 6708 | -17.83 | -19.86 | 22.16 | 7.53 | 3.18 | 0.33 |
| 2778 | 5410 | -17.64 | -19.59 | 21.48 | 6.06 | 1.59 | 0.07 |
| 2783 | 5294 | -16.91 | -18.86 | 22.41 | 6.42 | 1.98 | 0.06 |
| 2852 | 7451 | -17.24 | -19.36 | 23.17 | 7.89 | 2.52 | 0.11 |
| 2866 | 6992 | -17.99 | -19.79 | 22.36 | 6.35 | 3.54 | 0.06 |
| 2879 | 7387 | -16.97 | -18.85 | 21.88 | 3.68 | 1.81 | 0.08 |
| 2910 | 5136 | -17.96 | -19.21 | 20.55 | 3.75 | 1.61 | 0.20 |
| 2943 | 7289 | -16.33 | -18.02 | 23.57 | 8.05 | 1.37 | 0.51 |
| 2976 | 6693 | -16.66 | -18.29 | 21.55 | 3.30 | 1.51 | 0.33 |
| 2985 | 5291 | -16.41 | -17.57 | 21.81 | 3.60 | 1.40 | 0.38 |
| 3012 | 8064 | -17.72 | -19.48 | 23.06 | 9.85 | 2.11 | 0.47 |
| 3034 | 6439 | -16.65 | -18.24 | 23.20 | 5.86 | 2.09 | 0.14 |
| 3092 | 8247 | -17.71 | -19.69 | 21.78 | 4.08 | 3.01 | 0.07 |
| 3113 | 7601 | -17.26 | -18.84 | 21.42 | 3.26 | 1.47 | 0.21 |
| 3126 | 7905 | -17.62 | -19.55 | 21.49 | 5.46 | 1.50 | 0.47 |
| 3129 | 6729 | -16.87 | -18.91 | 22.08 | 5.61 | 2.05 | 0.43 |
| 3205 | 6196 | -17.02 | -18.51 | 21.39 | 3.62 | 1.43 | 0.30 |
| 3302 | 5714 | -17.12 | -18.56 | 20.91 | 2.94 | 1.76 | 0.23 |
| 3313 | 6231 | -17.11 | -18.79 | 20.57 | 2.04 | 2.95 | 0.04 |
| 3463 | 6618 | -16.68 | -18.80 | 22.54 | 8.92 | 2.16 | 0.68 |
| 3486 | 7604 | -17.35 | -18.81 | 21.73 | 2.99 | 3.00 | 0.13 |
| 3489 | 5507 | -16.44 | -18.59 | 23.42 | 8.39 | 2.90 | 0.16 |
| 3534 | 6411 | -17.50 | -18.97 | 21.15 | 4.57 | 2.01 | 0.57 |
| 3554 | 7125 | -17.74 | -20.10 | 22.74 | 8.27 | 3.76 | 0.03 |
| 3565 | 7140 | -16.50 | -18.10 | 22.47 | 4.52 | 2.01 | 0.46 |
| 3586 | 6681 | -16.61 | -18.27 | 21.63 | 2.56 | 2.52 | 0.07 |
| 3681 | 6942 | -16.87 | -18.53 | 21.18 | 2.56 | 1.38 | 0.06 |
| 3706 | 6892 | -17.25 | -18.96 | 20.46 | 1.90 | 4.00 | 0.18 |
| 3750 | 6339 | -16.60 | -17.91 | 20.96 | 1.91 | 1.64 | 0.12 |
| 3780 | 5080 | -16.30 | -18.46 | 22.54 | 7.15 | 2.44 | 0.41 |
| 3855 | 5722 | -16.40 | -18.19 | 22.38 | 4.67 | 1.96 | 0.20 |
| 3895 | 8535 | -17.60 | -19.05 | 21.43 | 3.52 | 0.96 | 0.21 |
| 3925 | 6448 | -16.72 | -18.85 | 21.33 | 3.46 | 1.36 | 0.06 |
| 4035 | 6665 | -16.30 | -18.07 | 23.22 | 5.13 | 1.98 | 0.06 |
| 4060 | 8686 | -17.81 | -18.85 | 22.94 | 6.05 | 1.10 | 0.20 |
| 4083 | 6202 | -16.81 | -18.54 | 22.31 | 6.28 | 2.40 | 0.56 |
| 4129 | 5991 | -16.01 | -17.82 | 22.19 | 3.04 | 2.27 | 0.04 |
| 4296 | 8352 | -17.42 | -19.09 | 21.43 | 3.02 | 1.61 | 0.08 |
| 4310 | 4366 | -15.35 | -17.01 | 22.17 | 3.00 | 3.16 | 0.25 |
| 4341 | 5434 | -17.01 | -18.68 | 20.29 | 3.14 | 1.80 | 0.53 |
| 4355 | 6205 | -16.41 | -18.19 | 21.45 | 2.80 | 1.34 | 0.05 |
| 4510 | 6609 | -16.26 | -18.17 | 21.23 | 3.12 | 1.18 | 0.43 |
| 4519 | 5638 | -16.81 | -18.60 | 21.26 | 3.38 | 2.35 | 0.24 |
| 4602 | 6444 | -16.56 | -19.09 | 23.78 | 13.69 | 3.20 | 0.52 |
| 4656 | 5809 | -16.86 | -18.68 | 20.76 | 3.09 | 1.31 | 0.24 |

Note. — Col. (1) GMP galaxy identification from the Coma catalog of Godwin et al. (1983). Col. (2) Velocity in km/s from Godwin et al. (1983). Col. (3) Absolute B magnitude from Godwin et al. (1983). Col. (4) Absolute R magnitude from the surface brightness profile fits of this work. Col. (5) effective surface brightness in R band. Col. (6) effective radius in arcsec. Col. (7) Sersic n parameter. Col. (8) Ellipticity.

Table 2. Structural parameters of the dS0 galaxies

| GMP (1) | V_{\odot} (2) | M_B (3) | M_R (4) | μ_e (5) | r_e (6) | n (7) | ϵ_b (8) | μ_0 (9) | h (10) | ϵ_d (11) |
|------------|--------------------|--------------|--------------|----------------|--------------|------------|---------------------|----------------|-------------|----------------------|
| 1594 | 5742 | -17.72 | -19.36 | 19.69 | 1.25 | 1.37 | 0.12 | 21.12 | 5.62 | 0.06 |
| 1931 | 7599 | -16.97 | -18.93 | 20.49 | 1.55 | 0.60 | 0.62 | 21.11 | 4.35 | 0.32 |
| 1975 | 5272 | -15.97 | -17.91 | 21.30 | 2.89 | 0.79 | 0.47 | 20.82 | 3.01 | 0.47 |
| 2194 | 8426 | -17.31 | -18.81 | 23.13 | 2.16 | 0.47 | 0.35 | 21.14 | 3.68 | 0.21 |
| 2421 | 8126 | -17.25 | -18.98 | 22.26 | 1.95 | 1.15 | 0.22 | 20.76 | 4.09 | 0.48 |
| 2565 | 7095 | -16.90 | -18.51 | 20.47 | 0.98 | 3.04 | 0.61 | 19.81 | 2.35 | 0.46 |
| 2692 | 7955 | -16.98 | -18.64 | 22.90 | 1.90 | 3.39 | 0.25 | 20.61 | 3.60 | 0.56 |
| 2736 | 4890 | -15.89 | -17.47 | 21.82 | 1.03 | 4.27 | 0.07 | 19.97 | 1.88 | 0.21 |
| 2753 | 7704 | -17.01 | -19.09 | 21.40 | 2.85 | 0.96 | 0.20 | 22.73 | 7.10 | 0.29 |
| 2800 | 7020 | -16.52 | -18.22 | 21.65 | 0.79 | 0.64 | 0.02 | 21.40 | 3.51 | 0.07 |
| 2863 | 4950 | -15.70 | -17.16 | 20.29 | 0.76 | 2.65 | 0.51 | 20.94 | 2.62 | 0.33 |
| 2914 | 7447 | -17.85 | -19.69 | 20.87 | 1.58 | 1.40 | 0.07 | 20.74 | 4.87 | 0.23 |
| 2923 | 8664 | -17.72 | -19.21 | 21.14 | 2.53 | 0.81 | 0.57 | 21.32 | 5.40 | 0.56 |
| 2960 | 5922 | -17.75 | -19.12 | 20.05 | 0.99 | 2.05 | 0.14 | 19.64 | 4.15 | 0.63 |
| 3017 | 6784 | -16.92 | -18.14 | 21.03 | 0.97 | 1.69 | 0.05 | 20.81 | 2.49 | 0.13 |
| 3292 | 4924 | -16.42 | -17.70 | 19.92 | 0.49 | 1.16 | 0.07 | 19.96 | 2.13 | 0.19 |
| 3298 | 6554 | -17.49 | -19.15 | 21.17 | 1.50 | 1.51 | 0.41 | 21.13 | 7.23 | 0.56 |
| 3339 | 6417 | -17.16 | -19.05 | 20.70 | 2.14 | 1.37 | 0.15 | 23.28 | 9.98 | 0.12 |
| 3433 | 5569 | -17.83 | -19.18 | 20.16 | 1.98 | 2.72 | 0.31 | 19.31 | 2.47 | 0.47 |
| 3475 | 8010 | -17.99 | -19.45 | 18.41 | 0.40 | 2.12 | 0.13 | 19.65 | 2.74 | 0.39 |
| 3481 | 7718 | -17.42 | -19.50 | 20.94 | 2.11 | 2.97 | 0.06 | 23.00 | 7.77 | 0.07 |
| 3522 | 5087 | -17.80 | -19.34 | 18.48 | 0.93 | 1.59 | 0.09 | 19.10 | 2.53 | 0.27 |
| 3640 | 7483 | -16.92 | -18.71 | 21.62 | 1.71 | 0.55 | 0.66 | 20.69 | 4.19 | 0.54 |
| 3707 | 7220 | -17.21 | -19.13 | 21.34 | 3.35 | 2.95 | 0.68 | 20.59 | 3.54 | 0.43 |
| 3882 | 6894 | -17.89 | -19.80 | 20.56 | 1.50 | 1.47 | 0.34 | 19.96 | 4.64 | 0.41 |
| 3943 | 5496 | -17.43 | -18.92 | 21.41 | 3.48 | 3.06 | 0.49 | 20.22 | 3.86 | 0.56 |
| 4348 | 7576 | -17.30 | -19.09 | 21.58 | 1.96 | 0.96 | 0.63 | 20.99 | 4.52 | 0.29 |
| 4372 | 6725 | -16.60 | -18.38 | 20.28 | 1.33 | 0.76 | 0.46 | 21.02 | 3.67 | 0.43 |
| 4420 | 8509 | -17.73 | -19.53 | 20.10 | 1.21 | 2.03 | 0.10 | 20.20 | 2.33 | 0.01 |

Note. — Col. (1) GMP galaxy identification from the Coma catalog of Godwin et al. (1983). Col. (2) Velocity in km/s from Godwin et al. (1983). Col. (3) Absolute B magnitude from Godwin et al. (1983). Col. (4) Absolute R magnitude from the surface brightness profile fits of this work. Col. (5) effective surface brightness in R band. Col. (6) effective radius in arcsec. Col. (7) Sersic n parameter. Col. (8) Ellipticity of the bulge. Col. (9) central surface brightness of the disc in R band. Col. (10) scale of the disk in arcsec. Col. (11) ellipticity of the disk.

Table 3. Velocity dispersion of the different types of galaxies

| Galaxy type | Gaussian fit | | | Directly | | Biweight estimator | |
|-------------|--|-----------------------------|----------|--|-----------------------------|--|-----------------------------|
| | $\langle v \rangle$ (km s $^{-1}$) | σ (km s $^{-1}$) | χ^2 | $\langle v \rangle$ (km s $^{-1}$) | σ (km s $^{-1}$) | $\langle v \rangle$ (km s $^{-1}$) | σ (km s $^{-1}$) |
| E | 6655 | 693 | 2.45 | 7096 | 1040 | 7057 ± 109 | 955 ± 145 |
| Sp | 6686 | 1252 | 4.42 | 7181 | 1161 | 7156 ± 238 | 1281 ± 158 |
| dE | 6329 | 979 | 3.23 | 6732 | 1023 | 6709 ± 126 | 1104 ± 96 |
| dS0 | 6622 | 1187 | 4.38 | 6819 | 1178 | 6881 ± 268 | 1288 ± 154 |
| dS0* | 6290 | 1068 | 0.39 | 6717 | 1147 | 6729 ± 308 | 1202 ± 171 |

Note. — (*) more reliable sub-sample of dS0 (see definition in Section 3.1)

Table 4. Structural parameters of the dS0 galaxies

| | dE | E | dS0 (bulges) | Spl (bulges) | Spe (bulges) | S0 (bulges) |
|-----------------|------------------|------------------|------------------|------------------|------------------|------------------|
| $< \mu_o >$ | 17.81 ± 0.21 | 12.87 ± 0.46 | 17.44 ± 0.45 | 16.08 ± 0.68 | 14.78 ± 0.68 | 12.80 ± 1.04 |
| $< \log(r_e) >$ | 0.26 ± 0.03 | 0.57 ± 0.09 | -0.21 ± 0.05 | -0.19 ± 0.06 | -0.01 ± 0.05 | 0.10 ± 0.06 |
| $< \log(n) >$ | 0.28 ± 0.02 | 0.58 ± 0.02 | 0.17 ± 0.05 | 0.26 ± 0.07 | 0.34 ± 0.05 | 0.49 ± 0.06 |